ORIGINS OF NATURAL REMANENT MAGNETISM

Of all the chapters in this book, this is "The Big Enchilada," the one you cannot skip. The physical processes leading to acquisition of natural remanent magnetism are presented here. Perhaps the most fundamental and fascinating aspect of paleomagnetism concerns the processes by which the geomagnetic field can be recorded at the time of rock formation and then retained over geological time. We want to remove any hint of "magic" from this aspect of paleomagnetism, preferably without removing the reader's natural astonishment that the processes actually work. Only the basic physical principles of each type of natural remanent magnetism are discussed. Some special topics in rock magnetism will be developed further in Chapter 8.

Many new concepts are presented, and some effort is required to follow the development. You will most likely have to read through this chapter more than once to see how these new concepts fit together. But effort at this point will be rewarded by ease of comprehension of principles developed in succeeding chapters. We start with a presentation of the theory of fine-particle ferromagnetism, which underlies all development of rock magnetism.

FERROMAGNETISM OF FINE PARTICLES

Rocks are assemblages of fine-grained ferromagnetic minerals dispersed within a matrix of diamagnetic and paramagnetic minerals. We are concerned with the magnetization of individual ferromagnetic grains on the one hand. But on the other hand, we must keep track of the magnetization of the rock, the entire assemblage of ferromagnetic grains plus matrix. It is useful to introduce a notation that distinguishes between magnetic parameters of individual ferromagnetic grains and magnetic parameters of entire samples. We adopt the convention that parameters for individual ferromagnetic grains are denoted by lowercase symbols, whereas parameters for the entire sample are designated by uppercase symbols. For example, the magnetization of an individual magnetite particle is designated $\boldsymbol{j}$ while the magnetization of the whole sample is designated $\boldsymbol{J}$.

A basic principle is that ferromagnetic particles have various energies which control their magnetization. No matter how simple or complex the combination of energies may become, the grain seeks the configuration of magnetization which minimizes its total energy.

Magnetic domains

The first step is to introduce concepts and observations of magnetic domains. Consider the spherical particle of ferromagnetic material with uniform magnetization shown in Figure 3.1a. Atomic magnetic moments can be modeled as pairs of magnetic charges (as in Figure 1.1a). Magnetic charges of adjacent atoms cancel internal to the particle but produce a magnetic charge distribution at the surface of the particle. For a spherical particle, one hemisphere has positive charge and the other has negative charge. There is energy stored in this charge distribution because of repulsion between adjacent charges. This is *magnetostatic energy*, e_m.

We will soon develop an equation to determine the magnetostatic energy for a uniformly magnetized grain. At this point, all we need to know is that, for a grain with uniform magnetization j, e_m is proportional to j^2.

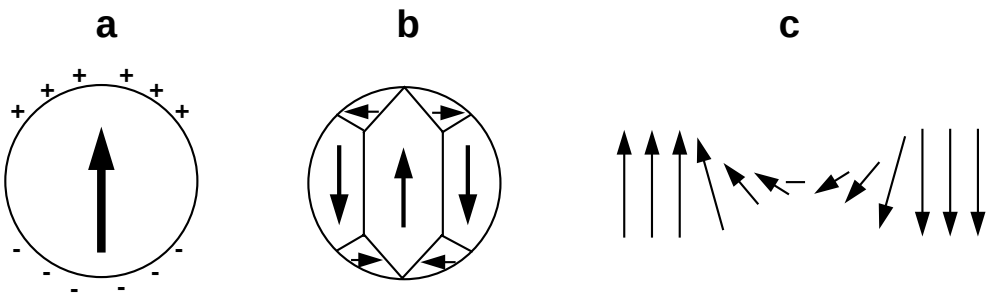

Figure 3.1 (**a**) Uniformly magnetized sphere of ferromagnetic material. The direction of saturation magnetization $\boldsymbol{j_s}$ is shown by the arrow; surface magnetic charges are shown by plus and minus signs. (**b**) Sphere of ferromagnetic material subdivided into magnetic domains. Arrows show the directions of $\boldsymbol{j_s}$ within individual magnetic domains; planes separating adjacent magnetic domains are domain walls. (**c**) Rotation of atomic magnetic moments within a domain wall. Arrows indicate the atomic magnetic moments which spiral in direction inside the domain wall.

A uniformly magnetized ferromagnetic grain has $j = j_s$, and magnetostatic energy is extreme for materials with high j_s.

Formation of *magnetic domains* as shown in Figure 3.1b decreases magnetostatic energy because the percent of surface covered by magnetic charges is reduced and charges of opposite sign are adjacent rather than separated. Internal to any individual domain, the magnetization is j_s, but the entire grain has net magnetization, $j << j_s$. Magnetite grains of diameter $d > 10$ μm contain scores of domains and are referred to as *multidomain* (MD) grains. The region separating domains is the *domain wall* (Figure 3.1c). Because of exchange energy between adjacent atoms, atomic magnetic moments gradually spiral through the domain wall, which has both finite energy and finite width (~1000 Å for magnetite).

Single-domain grains

With decreasing grain size, the number of magnetic domains decreases. Eventually, the grain becomes so small that the energy required to make a domain wall is larger than the decrease in magnetostatic energy resulting from dividing the grain into two domains. Below this particle size, it is not energetically favorable to subdivide the grain into numerous domains. Instead, the grain will contain only one domain. These grains are referred to as *single-domain* (SD) grains, and magnetic properties of SD grains are dramatically different from those of MD grains.

The grain diameter below which particles are single domain is the *single-domain threshold grain size* (d_0). This size depends upon factors including grain shape and saturation magnetization, j_s. Ferromagnetic materials with low j_s have little impetus to form magnetic domains because magnetostatic energy is low. Thus, hematite (with j_s = 2 G) is SD up to grain diameter (d_0) = 15 μm, so a large portion of hematite encountered in rocks is single domain. However, magnetite has much higher j_s and only fine-grained magnetite is SD. Theoretical values for d_0 in parallelepiped-shaped particles of magnetite are shown in Figure 3.2.

Cubic magnetite particles must have $d < 0.1$ μm to be SD, but elongated SD particles can be upward to 1 μm in length. In discussion of magnetic mineralogy in Chapter 2, examples of fine-grained magnetites were presented. So we know that fine-grained magnetites do exist and that crystals of elongate habit are common. Igneous rocks and their derivative sediments generally have some fraction of magnetite grains within the SD grain-size range.

SD grains can be very efficient carriers of remanent magnetization. To understand the behavior of SD grains, we must become familiar with energies that collectively control the direction of magnetization in a SD grain. These energies are introduced individually, then the collective effects are considered to explain hysteresis parameters.

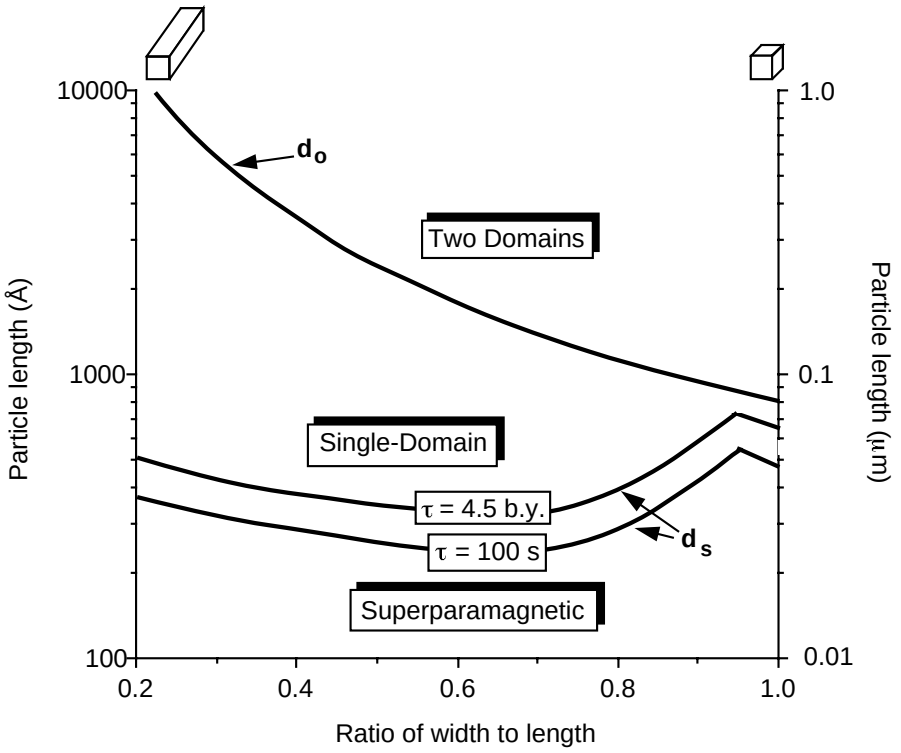

Figure 3.2 Size and shape ranges of single-domain, superparamagnetic, and two-domain configurations for parallelepipeds of magnetite at 290°K. Particle lengths are indicated in angstroms (Å) on the left ordinate and in microns (μm) on the right ordinate; shape is indicated by the ratio of width to length; cubic grains are at the right-hand side of diagram; progressively elongate grains are toward the left; the curve labeled d_0 separates the single-domain size and shape field from the size and shape distribution of grains that contain two domains; curves labeled d_s are size and shape distribution of grains that have τ = 4.5 b.y. and τ = 100 s; grains with sizes below d_s curves are superparamagnetic. Redrawn after Butler and Banerjee (*J. Geophys. Res.*, v. 80, 4049–4058, 1975).

Interaction energy

There is an *interaction energy*, e_H, between the magnetization of individual ferromagnetic particles, $\boldsymbol{j}$, and an applied magnetic field, $\boldsymbol{H}$. This energy essentially represents the interaction between the magnetic field and the atomic magnetic moments (Equation (1.4)) integrated over the volume of the ferromagnetic grain.

The interaction energy describes how the magnetization of a ferromagnetic grain is influenced by an externally applied magnetic field. (In detail, one has to deal with balancing torques on the magnetization, $\boldsymbol{j}$, from the external field against internal energies that resist rotation of $\boldsymbol{j}$. But a simplified approach will serve our purpose.) The interaction energy, e_H, is given by

$$e_H = \frac{-\mathbf{j}\cdot\mathbf{H}}{2} \tag{3.1}$$

This is an energy density (energy per unit volume) and applies to both SD and MD grains.

Single-domain grains have uniform magnetization with $j = j_s$. So application of a magnetic field cannot change the intensity of magnetization but can rotate $\boldsymbol{j_s}$ toward the applied field. However, there are resistances to rotation of $\boldsymbol{j_s}$. These resistances are referred to as *anisotropies* and lead to energetically preferred directions for $\boldsymbol{j_s}$ within individual SD grains. The dominant anisotropies are *shape anisotropy* and *magnetocrystalline anisotropy*.

The internal demagnetizing field

As discussed above, a surface magnetic charge results from magnetization of a ferromagnetic substance directed toward the grain surface. For a spherical SD grain, the magnetic charge distribution is shown in Figure 3.3a. The magnetic field produced by this grain can be determined from the magnetic charge distribution. For a uniformly magnetized sphere, the resulting external magnetic field is a dipole field (Equations (1.12)–(1.15)). But the magnetic charge distribution also produces a magnetic field internal to the ferromagnetic grain. This internal magnetic field is shown in Figure 3.3b and is called the *internal demagnetizing field* because it opposes the magnetization of the grain.

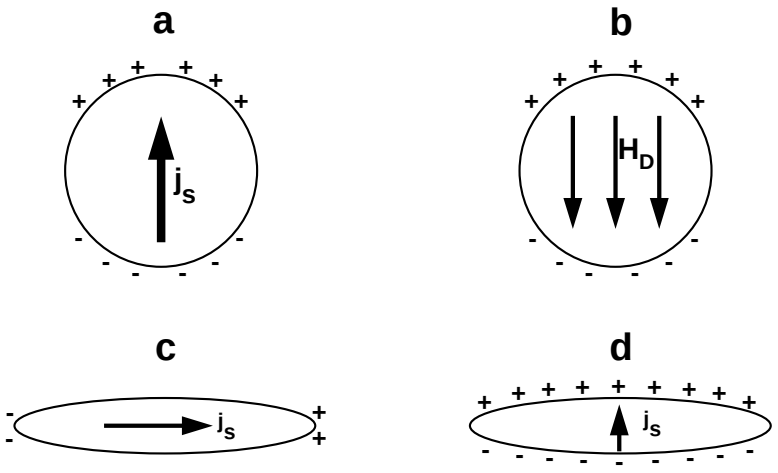

Figure 3.3 (**a**) Surface magnetic charge distribution resulting from uniform magnetization of a spherical ferromagnetic grain. The arrow indicates the direction of saturation magnetization $\boldsymbol{j_S}$; plus and minus signs indicate surface magnetic charges. (**b**) Internal demagnetizing field, $\boldsymbol{H_D}$, resulting from the surface magnetic charge of a uniformly magnetized sphere. $\boldsymbol{H_D}$ is uniform within the grain. (**c**) Surface magnetic charge produced by magnetization of an SD grain along the long axis of the grain. The arrow indicates the direction of saturation magnetization $\boldsymbol{j_S}$; plus and minus signs indicate surface magnetic charges; note that magnetic charges are restricted to the ends of the grain. (**d**) Surface magnetic charge produced by magnetization of an SD grain perpendicular to the long axis of the grain. The arrow indicates the direction of saturation magnetization $\boldsymbol{j_S}$; plus and minus signs indicate surface magnetic charges; note that magnetic charges appear over the entire upper and lower surfaces of the grain.

For uniformly magnetized ellipsoids, the internal demagnetizing field, $\boldsymbol{H_D}$, is given by

$$\boldsymbol{H_D} = -N_D \boldsymbol{j} \tag{3.2}$$

where $\boldsymbol{j}$ is the magnetization of the grain and N_D is the *internal demagnetizing factor*. The internal demagnetizing factor is a coefficient relating the strength of the internal demagnetizing field to the magnetization. The internal demagnetizing factor along any particular direction is proportional to the percentage of the grain surface covered by magnetic charges when the grain is magnetized in that direction. If you erect a Cartesian (x, y, z) coordinate system inside the ferromagnetic grain, the internal demagnetizing factors along the three orthogonal directions must sum to 4π:

$$N_{Dx} + N_{Dy} + N_{Dz} = 4\pi \tag{3.3}$$

where N_{Dx} is the internal demagnetizing factor along the x direction and so on.

Now consider a spherical SD grain (Figure 3.3a). No matter what direction the magnetization points, the same percentage of the grain surface gets covered by magnetic charges. This means that

$$N_{Dx} = N_{Dy} = N_{Dz} = \frac{4\pi}{3} \tag{3.4}$$

So the internal demagnetizing field for a spherical SD grain is

$$\mathbf{H_D} = -\frac{4\pi}{3}\mathbf{j} = -\frac{4\pi}{3}\mathbf{j_s} \tag{3.5}$$

With this result, we can show how to determine the magnetostatic energy. For a uniformly magnetized ellipsoid, the magnetostatic energy is the interaction energy of the internal demagnetizing field with the magnetization in the grain:

$$e_m = -\frac{\mathbf{j}\cdot\mathbf{H}}{2} = -\frac{\mathbf{j}\cdot\mathbf{H_D}}{2} = -\frac{(\mathbf{j_s})\cdot(-N_D\ \mathbf{j_s})}{2} = \frac{N_D\ j_s^2}{2} \tag{3.6}$$

This expression makes it clear why SD grains have high magnetostatic energy, especially if j_s is large.

Shape anisotropy

We can also use the internal demagnetizing field and magnetostatic energy to introduce *shape anisotropy*. The origin of shape anisotropy is illustrated in Figures 3.3c and 3.3d. A highly elongate ferromagnetic grain has much lower magnetostatic energy if magnetized along its length (Figure 3.3c) rather than perpendicular to its length (Figure 3.3d). This is because the percentage of surface covered by magnetic charges is small when $\boldsymbol{j_s}$ points along the long dimension of the grain (Figure 3.3c). But magnetization perpendicular to the long axis leads to a substantial surface charge (Figure 3.3d). So the internal demagnetizing factor, N_{Dl}, along the long axis is much less than the internal demagnetizing factor, N_{Dp}, perpendicular to the long axis.

We can use Equation (3.6) to determine the difference in magnetostatic energy between magnetization along the long axis and magnetization perpendicular to the long axis. The difference in magnetostatic energy is

$$\Delta e_m = \frac{(N_{Dp} - N_{Dl}) j_s^{\,2}}{2} = \frac{\Delta N_D\ j_s^{\,2}}{2} \tag{3.7}$$

where ΔND *is* the difference in demagnetizing factors between short and long axes. This difference in magnetostatic energy represents an energy barrier to rotation of $\boldsymbol{j_s}$ through the perpendicular direction. In the absence of other influences, the grain will have $\boldsymbol{j_s}$ along the long axis.

To force $\boldsymbol{j_s}$ over the magnetostatic energy barrier, an external magnetic field must result in an interaction energy, e_H, which exceeds the energy barrier, Δe_m. By using Equations (3.1) and (3.7) the required interaction energy is

$$e_H = \frac{j_s\ H}{2} > \Delta e_m = \frac{\Delta N_D\ j_s^{\,2}}{2} \tag{3.8}$$

The required magnetic field is given by

$$h_c = \Delta N_D\ j_s \tag{3.9}$$

The magnetic field h_c required to force $\boldsymbol{j_s}$ over the energy barrier of an individual SD grain is the *microscopic coercive force*. This microscopic coercive force is a measure of the energy barrier to rotation of $\boldsymbol{j_s}$ in a SD grain and will be used extensively in models for acquisition of remanent magnetization. For elongate grains of magnetite, microscopic coercive force is dominated by shape anisotropy. Maximum shape anisotropy is displayed by needle-shaped grains for which ΔN_D in Equation (3.9) is 2π. Using j_s = 480 G leads to maximum coercive force for SD magnetite at room temperature of ~3000 Oe (300 mT).

Magnetocrystalline anisotropy

For equant SD particles (no shape anisotropy) or SD particles of ferromagnetic materials with low j_S, *magnetocrystalline anisotropy* dominates the microscopic coercive force. *Magnetocrystalline easy directions* of magnetization are crystallographic directions along which magnetocrystalline energy is minimized. An example of magnetization along different crystallographic directions in a single crystal of magnetite is shown in Figure 3.4. Magnetization is more easily achieved along the [111] magnetocrystalline easy direction. The origin of magnetocrystalline anisotropy is the dependence of exchange energy on crystallographic direction of magnetization.

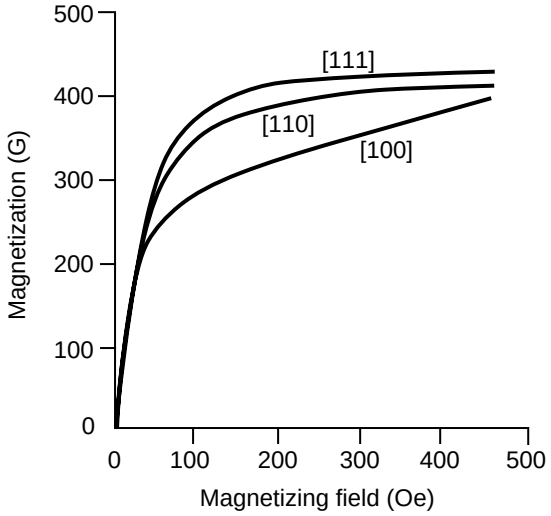

Figure 3.4 Magnetization of a single crystal of magnetite as a function of the magnetizing field. Magnetization curves are labeled indicating the crystallographic direction of the magnetizing field; [111] is the magnetocrystalline easy direction; [100] is the magnetocrystalline hard direction. Redrawn after Nagata (*Rock Magnetism*, Maruzen Ltd., Tokyo, 350 pp, 1961).

It is simplest to understand magnetocrystalline anisotropy by considering a material with *uniaxial magnetocrystalline energy*, e_a. Such a material contains one axis of minimum magnetocrystalline energy, and e_a is given by

$$e_a = \mathrm{K}\sin^2\theta \tag{3.10}$$

where K is the magnetocrystalline constant and θ is the angle between $\boldsymbol{j_s}$ and the magnetocrystalline easy direction. There is an energy barrier to rotation of $\boldsymbol{j_s}$ through the *magnetocrystalline hard direction* where θ = 90° and e_a = K. To force $\boldsymbol{j_s}$ through this energy barrier, e_H > K is required. The resulting microscopic coercive force for an individual SD particle is

$$h_c = 2\mathrm{K} / j_s \tag{3.11}$$

Magnetocrystalline anisotropy is the dominant source of microscopic coercive force in hematite because K is large and j_S is small. The resulting h_c can exceed 10^4 Oe (1 T) for SD particles of hematite.

Hysteresis in single-domain grains

Consider a synthetic sample composed of 5% by volume dispersed magnetite particles in a diamagnetic matrix. The magnetite grains are all elongate single-domain grains, and the directions of long axes of the grains are randomly distributed. Typical values of hysteresis parameters for such a sample (at room temperature) are shown in Figure 3.5a.

Magnetization of individual ferromagnetic particles, $\boldsymbol{j_n}$, adds vectorially to yield net magnetization for the sample given by

$$\mathbf{J} = \frac{\sum_n v_n \, \mathbf{j_n}}{\text{sample volume}} \tag{3.12}$$

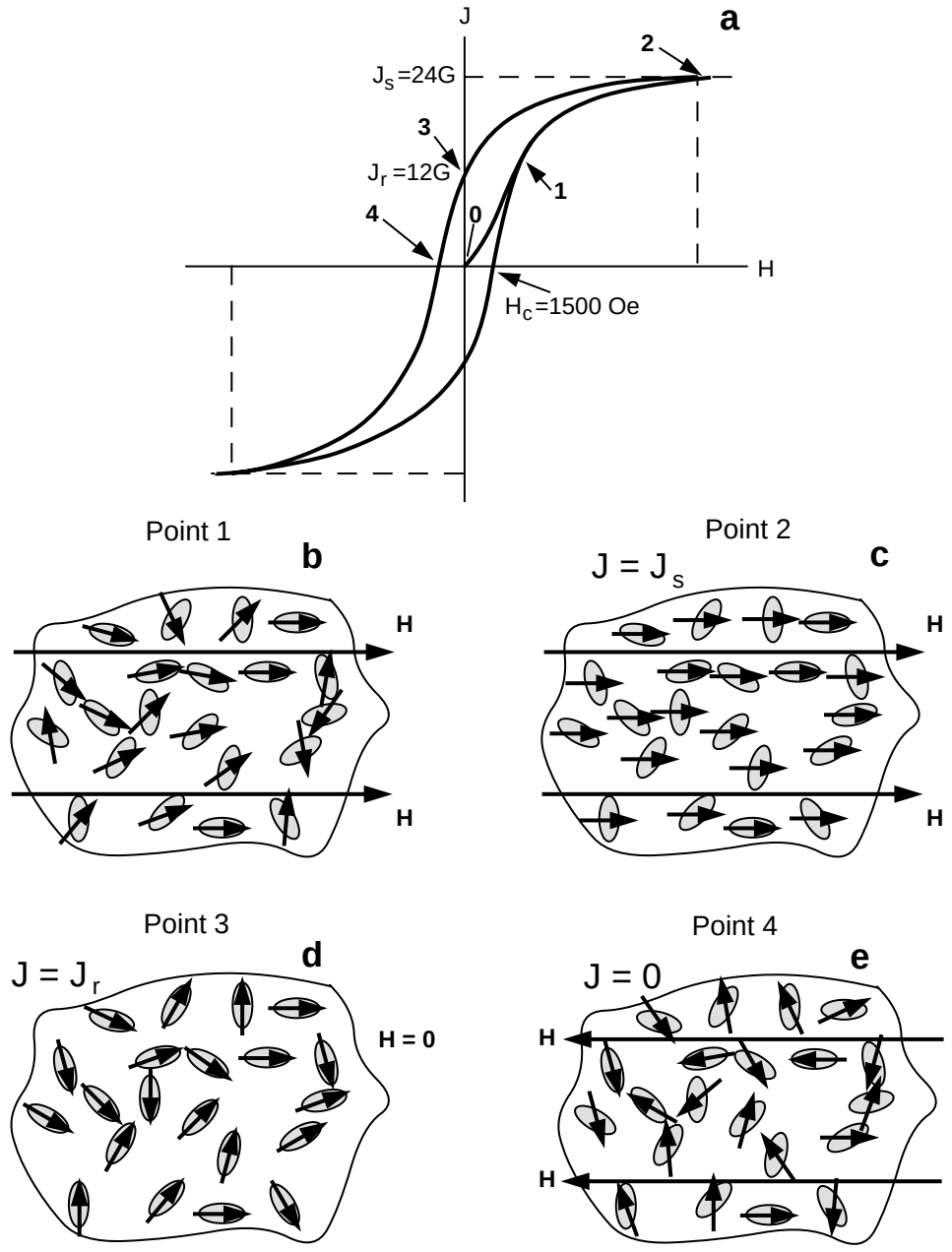

Figure 3.5 (**a**) Hysteresis loop for synthetic sample containing 5% by volume of dispersed elongate SD magnetite particles. The saturation magnetization of the sample is J_S; the remanent magnetization of the sample is J_r; the bulk coercive force is H_C; the points labeled are referred to in text and illustrated below. (**b**) Magnetization directions within SD grains at point 1 on hysteresis loop. Stippled ovals are schematic representations of elongate SD magnetite grains; arrows indicate direction of $\boldsymbol{j_S}$ for each SD grain; $\boldsymbol{H}$ is the magnetizing field; note that $\boldsymbol{j_S}$ of each grain is rotating toward $\boldsymbol{H}$. (**c**) Magnetization directions within SD grains at point 2 on hysteresis loop. Sample is at saturation magnetization J_S; note that $\boldsymbol{j_S}$ of every grain is aligned with $\boldsymbol{H}$. (**d**) Magnetization directions within SD grains at point 3 on hysteresis loop. The magnetizing field has been removed; sample magnetization is remanent magnetization J_r; note that $\boldsymbol{j_S}$ of each grain has rotated back to the long axis closest to the saturating magnetic field, which was directed toward the right. (**e**) Magnetization directions within SD grains at point 4 on hysteresis loop. The sample has magnetization $J = 0$; note that $\boldsymbol{j_S}$ of every grain has been slightly rotated toward the magnetizing field $\boldsymbol{H}$ (now directed toward the left).

where v_n is the volume of an individual ferromagnetic particle and $v_n \boldsymbol{j_n}$ is the magnetic moment of an individual SD grain. It is the magnitude of this net magnetization that is measured in the hysteresis experiment. If the sample has not previously been exposed to a magnetizing field, $J = 0$ because the magnetization ($= j_S$) of SD grains is randomly directed.

Application of the initial magnetizing field (in an arbitrarily defined positive direction) leads to net magnetization acquired parallel to the field along the path 0–1–2. As the field is applied, $\boldsymbol{j_S}$ of each SD grain begins to rotate toward the applied magnetic field because of the interaction energy, e_H. Directions of $\boldsymbol{j_S}$ are shown schematically in Figure 3.5b for point 1 on the hysteresis loop.

If the applied field is increased to a sufficient level, all grains will have $\boldsymbol{j_S}$ aligned with the field (Figure 3.5c). This is point 2 of Figure 3.5a, where the sample reaches its *saturation magnetization*, J_S. The magnetizing field required to drive the sample to saturation is that required to overcome the magnetostatic energy barrier given by Equation (3.7). For elongate SD grains of magnetite, this saturating field is ~3000 Oe (300 mT).

For this sample containing 5% by volume of magnetite, the saturation magnetization can be computed by using Equation (3.12):

$$J_S = \frac{\sum_n j_S\, v_n}{\text{sample volume}} = \frac{j_S \sum_n v_n}{\text{sample volume}}$$

$$= j_S \frac{\text{total magnetite volume}}{\text{sample volume}}$$

$$= j_S \text{ (volume fraction magnetite)} = \text{(480 G) (0.05)}$$

$$= \text{24 G } (2.4 \times 10^4 \text{ A/m})$$

So saturation magnetization of the sample depends linearly on concentration of the ferromagnetic mineral.

Removal of the magnetizing field causes J to decrease along the path 2–3. During removal of the magnetizing field, $\boldsymbol{j_S}$ of individual SD grains rotates to the nearest long axis of the grain because that direction minimizes magnetostatic energy. After removal of the magnetizing field, a *remanent magnetization*, J_r, remains. Directions of $\boldsymbol{j_S}$ for the SD grains at point 3 are shown schematically in Figure 3.5d. Integrating the components of $\boldsymbol{j_S}$ over a random directional distribution of long axes yields $J_r = J_S / 2$. The ratio J_r / J_S is often taken as a measure of efficiency in acquiring remanent magnetization and is 0.5 for this assemblage of elongate SD grains with dominant shape anisotropy. Likewise an assemblage of SD grains with dominant uniaxial magnetocrystalline anisotropy and randomly directed magnetocrystalline easy axes would have $J_r / J_S = 0.5$.

To force J back to zero, an opposing magnetic field must be applied. J decreases along the path 3–4, and the magnetic field required to drive J to zero is the *bulk coercive force*, H_c. Directions of $\boldsymbol{j_S}$ for SD grains at point 4 are shown in Figure 3.5e. Integration of the effects of interaction energy and magnetostatic energy over an assemblage of randomly oriented elongate grains yields $H_c = h_c / 2$, where h_c is microscopic coercive force for an individual SD grain (Equation (3.9)). For the sample with elongate SD magnetite grains, $H_c \approx$ 1500 Oe (150 mT). Similarly, for an assemblage of SD grains with dominant magnetocrystalline energy, $H_c = h_c / 2$, with h_c given by Equation (3.11). For an assemblage of hematite grains, H_c can reach 5000 Oe (500 mT).

Notice that H_c does not depend on the concentration of ferromagnetic material. This is because h_c depends on energy balances within individual SD grains and H_c depends only on h_c; concentration of the grains is not involved. The hysteresis loop in Figure 3.5a is completed by driving the sample to saturation in the negative direction, then cycling back to saturation in the positive direction (Figure 3.5a). This example shows how assemblages of SD ferromagnetic grains are efficient in acquiring remanent magnetization and resistant to demagnetization; both properties are obviously desirable for paleomagnetism.

Rock samples containing titanomagnetite as the dominant ferromagnetic mineral rarely have H_c or J_r / J_s approaching the high values that we determined for this synthetic sample. Remember that rocks generally have a large percentage of MD grains and/or pseudo-single-domain grains (defined below); and these larger grains have lower h_c and lower J_r / J_s.

Hysteresis of multidomain grains

Application of a magnetic field to a MD grain produces preferential growth of domains with magnetization parallel to the field. If the applied field is sufficiently strong, domain walls are destroyed, and magnetization reaches saturation ($j = j_s$). On removal of the magnetizing field, domains re-form and move back towards their initial positions. However, because of lattice imperfections and internal strains, domain wall energy is a function of position (Figure 3.6). Rather than returning to initial positions, domain walls settle in energy minima near their initial positions, and a small remanent magnetization results. But only a small magnetic field is required to drive the domain walls back to the zero moment positions, so coercive force of MD ferromagnetic particles is modest. In addition, magnetization of MD particles tends to decay with time (domain walls can easily pass over energy barriers), and these particles are much less effective as recorders of paleomagnetism than are SD grains.

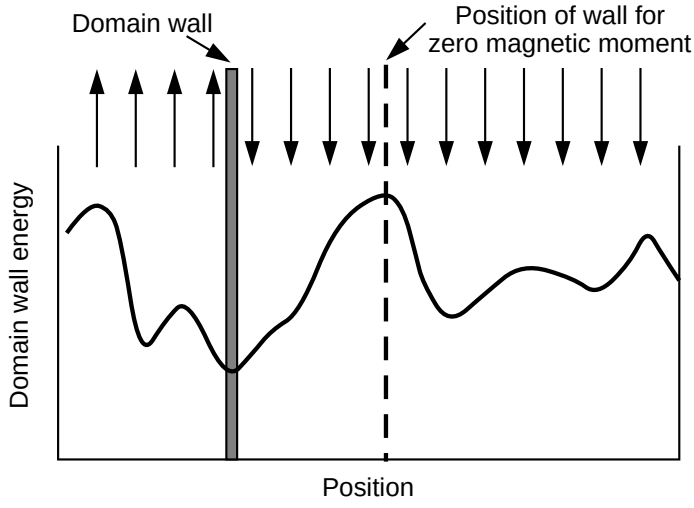

Figure 3.6 Domain wall energy versus position. The solid curve schematically represents domain wall energy; arrows show the direction of $\boldsymbol{j_s}$ within the domains; the domain wall is shown by the stippled region; the position of the domain wall that yields net $J = 0$ is shown by the dashed line. Redrawn after Stacey and Banerjee (1974).

Pseudo-single-domain grains

No sharp boundary exists between large SD grains and small multidomain grains. Instead, there is an interval of grain sizes exhibiting intermediate J_r / J_s and intermediate h_c. These grains are referred to as *pseudo-single-domain* (PSD) grains and are important in understanding magnetizations of rocks containing magnetite or titanomagnetite. The PSD grain-size interval for magnetite is approximately 1–10 μm. Grains in this size range contain a small number of domains and can have substantial magnetic moment. They can also exhibit significant coercivity and time stability of remanent magnetism. Grain-size distributions of many igneous and sedimentary rocks peak within the magnetite PSD field but have only a small percentage of particles within the true SD field. Accordingly, PSD grains can be important carriers of paleomagnetism. We will consider PSD grains at several points in our discussion of natural remanent magnetization.

Magnetic relaxation and superparamagnetism

In the above discussion, effects of magnetic fields on rotation of $\boldsymbol{j_s}$ in SD particles were considered. Thermal activation also can lead to rotation of $\boldsymbol{j_s}$ over energy barriers. *Magnetic relaxation*, in which remanent magnetization of an assemblage of SD grains decays with time, is the most straightforward effect of thermal activation. This relaxation is schematically illustrated in Figure 3.7a.

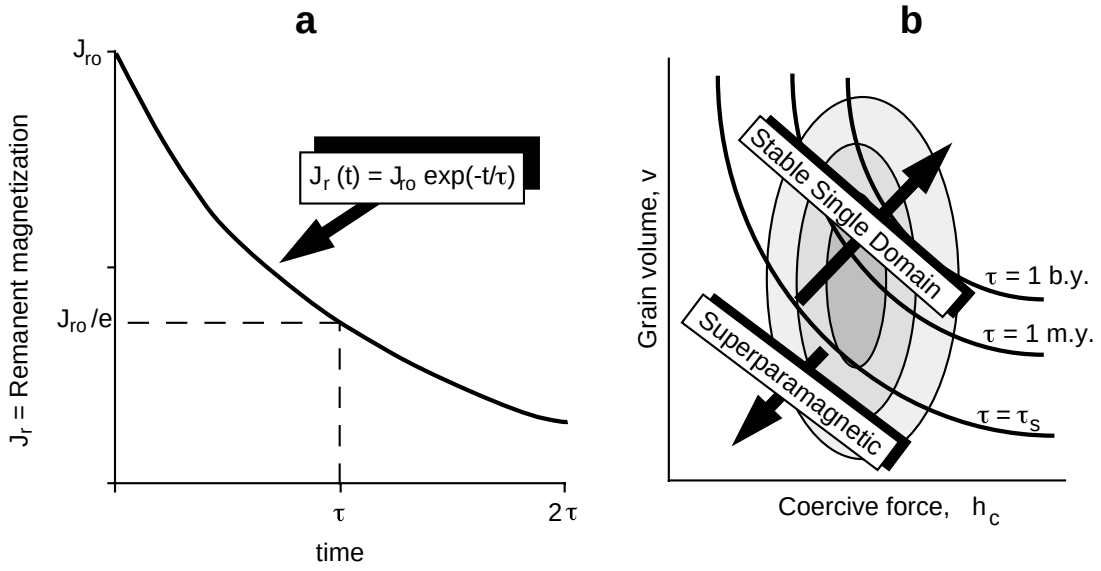

Figure 3.7 (**a**) Magnetic relaxation in an assemblage of SD ferromagnetic grains. Initial magnetization J_{r0} decays to J_{r0}/e in time τ. (**b**) Relaxation times of SD grains on diagram plotting SD grain volume, v, against SD grain microscopic coercive force, h_c. Lines of equal τ are lines of equal product vh_c; grains with short τ plot toward the lower left; grains with long τ plot toward the upper right; superparamagnetic grains with $\tau < \tau_S$ plot to the lower left of $\tau = \tau_S$ line; stable SD grains with $\tau > \tau_S$ plot to upper right of $\tau = \tau_S$ line; the schematic contoured plot of population of SD grains is shown by the stippled regions.

Exponential decay of remanent magnetization, $J_r(t)$, after removal of the magnetizing field is

$$J_r(t) = J_{r0} \exp(-t/\tau) \tag{3.13}$$

where J_r = initial remanent magnetization
t = time (s)
τ = charact*eristic relaxation time* (s), after which $J_r = J_{r0} / e$.

Magnetic relaxation was studied by Louis Néel, who showed that the characteristic relaxation time is given by

$$\tau = \frac{1}{\mathrm{C}} \exp\left(\frac{v\, h_c\, j_s}{2\mathrm{k}T} \right) \tag{3.14}$$

where C = *frequency factor* $\approx 10^8$ s^{-1}
v = volume of SD grain
h_c = microscopic coercive force of SD grain
j_s = saturation magnetization of the ferromagnetic material
kT = thermal energy

In Equation (3.14), the product vj_sh_c is an energy barrier to rotation of $\boldsymbol{j_s}$ and is called the *blocking energy*. But thermal energy (kT) can cause oscillations of $\boldsymbol{j_s}$. So the relaxation time is controlled by the ratio of blocking energy to thermal energy.

Relaxation times vary over many orders of magnitude. SD grains with short relaxation times are referred to as *superparamagnetic*. A superparamagnetic grain is ferromagnetic with attendant strong magnetization. But remanent magnetization in an assemblage of these grains is unstable; it will decay to zero very soon after removal of the magnetizing field (much like paramagnetic materials that "decay" instantaneously).

From Equation (3.14) it is clear that relaxation time for SD grains of a given material at a constant temperature depends on grain volume, v, and microscopic coercive force, h_c. It is convenient to plot distributions of grains on a *volume-versus-coercive force diagram* as shown in Figure 3.7b. Grains with low product (vh_c) plot in the lower left portion of the diagram and have low relaxation time. Grains with high product (vh_c) plot in the upper right and have long relaxation time. Lines of equal τ in v–h_c space are hyperbolas of equal product (vh_c). These diagrams prove useful in understanding the formation of several types of natural remanent magnetism and in understanding thermal demagnetization.

By definition, superparamagnetic grains are those grains whose remanence relaxes quickly. A convenient *critical relaxation time,* τ_s, for purposes of laboratory experiments may be taken as 100 s. It is possible to determine the size and shape of SD grains with $\tau < \tau_s$. This grain size is known as the *superparamagnetic threshold* (d_s). At 20°C (= 293°K), d_s for hematite and for equant grains of magnetite is about 0.05 μm. For elongate SD magnetite grains (with h_c controlled by shape anisotropy), size and shape of grains with τ =100 s is shown in Figure 3.2. For instance, a magnetite grain with a width:length ratio of 0.2 and length of 0.04 μm has τ =100 s and is (by definition of τ_s = 100 s) at the superparamagnetic threshold.

Effective paleomagnetic recorders must have relaxation times on the order of geological time. So it might be more appropriate to choose $\tau_s = 4.5 \times 10^9$ yr as the relevant relaxation time. The size and shape dependence of elongated magnetite particles with this relaxation time is also shown in Figure 3.2. Assemblages of SD grains with $d_s < d < d_0$ are considered to be within the *stable SD grain-size range.* These grains have desirable SD properties (high J_r / J_s and high h_c) and also have the required long relaxation time. The stable SD grain-size field for magnetite (Figure 3.2) is extremely narrow for equant particles but significant for elongated grains.

For hematite, the stable SD grain-size range is large, extending from d_s = 0.05 μm to d_0 = 15 μm. So a large percentage of hematite grains will be stable SD grains. In most rocks, a significant percentage of ferromagnetic grains will fall within the stable SD grain-size field. These grains are highly effective carriers of paleomagnetism. We will introduce many concepts of paleomagnetism by utilizing the properties of stable SD grains.

Blocking temperatures

Relaxation time has strong temperature dependence. Several parameters (besides temperature itself) appear in the argument of the exponential function in Equation (3.14). Temperature dependence of j_s (which goes to zero at T_c, the Curie temperature) is shown for both magnetite and hematite in Figure 2.3. Coercive force also depends upon temperature. For coercive force controlled by shape anisotropy, h_c is proportional to j_s, whereas coercive force controlled by magnetocrystalline anisotropy is proportional to j_s^n, with $n > 3$.

Relaxation times for an elongate SD magnetite grain with length 0.1 μm and width 0.02 μm are plotted in Figure 3.8 in semi-log format. Relaxation time is less than 1 microsecond at 575°C but exceeds the age of the earth at 510°C! If we choose 100 s as the critical relaxation time, τ_s, this grain changes behavior from superparamagnetic to stable SD at 550°C. The temperature at which this transition occurs is the *blocking temperature* (T_B). Between T_c and T_B, the grain is ferromagnetic, but remanent magnetization in an assemblage of these grains will decay quickly. Below the blocking temperature, τ exceeds τ_s and is increasing rapidly during continued cooling. Remanent magnetism formed at or below T_B can be stable, especially if temperature is decreasing.

Designation of blocking temperature depends on the choice of critical relaxation time. If we choose 10^3 yr as a more geologically relevant critical relaxation time, the corresponding blocking temperature would be 530°C rather than 550°C using τ_s = 100 s. The important consideration now is that relaxation time has extraordinary dependence on temperature; SD grains that have $\tau > 10^9$ yr at 20°C can be superparamagnetic at elevated temperature.

Rocks have distributions of ferromagnetic grain sizes and shapes yielding distributions of T_B between T_c and surface temperatures. The strong dependence of relaxation time on temperature and the transition in

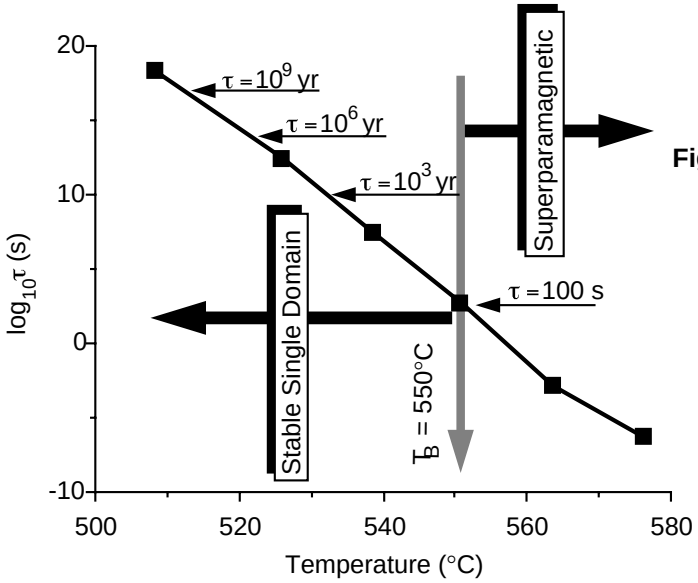

Figure 3.8 Semi-log plot of relaxation time, τ, of a SD magnetite grain as function of temperature. Key relaxation times are labeled; blocking temperature (T_B) is shown by stippled arrow; SD grain is superparamagnetic ($\tau < \tau_s$ =100 s) at $T > T_B$ = 550°C and "stable" ($\tau > \tau_s$ = 100 s) for $T < T_B$.

behavior from superparamagnetic above T_B to stable SD below T_B are critical to understanding acquisition of thermoremanent magnetism.

NATURAL REMANENT MAGNETISM (NRM)

In situ magnetization of rocks is the vector sum of two components:

$$\boldsymbol{J} = \boldsymbol{J_i} + \boldsymbol{J_r} \tag{3.15}$$

where $\boldsymbol{J_i}$ is the induced magnetization and $\boldsymbol{J_r}$ is the natural remanent magnetism. Bulk susceptibility, χ, is the net susceptibility resulting from contributions of all minerals but usually dominated by the ferromagnetic minerals. Presence of the local geomagnetic field, $\boldsymbol{H}$, produces the induced magnetization:

$$\boldsymbol{J_i} = \chi \boldsymbol{H} \tag{3.16}$$

This induced magnetization usually parallels the local geomagnetic field and can be the dominant component for many rock types. However, acquisition of induced magnetization is a reversible process without memory of past magnetic fields. It is the remanent magnetization that is of concern in paleomagnetism.

Natural remanent magnetization (NRM) is remanent magnetization present in a rock sample prior to laboratory treatment. NRM depends on the geomagnetic field and geological processes during rock formation and during the history of the rock. NRM typically is composed of more than one component. The NRM component acquired during rock formation is referred to as *primary NRM* and is the component sought in most paleomagnetic investigations. However, *secondary NRM* components can be acquired subsequent to rock formation and can alter or obscure primary NRM. The secondary components of NRM add vectorially to the primary component to produce the total NRM:

$$\textbf{NRM} = \textbf{primary NRM} + \textbf{secondary NRM} \tag{3.17}$$

The three basic forms of primary NRM are (1) *thermoremanent magnetization*, acquired during cooling from high temperature; (2) *chemical remanent magnetization*, formed by growth of ferromagnetic grains below the Curie temperature; and (3) *detrital remanent magnetization*, acquired during accumulation of sedimentary rocks containing detrital ferromagnetic minerals. In the sections below, these forms of NRM are examined. The objective is to explain how primary NRM can record the geomagnetic field present during rock formation and, under favorable conditions, retain that recording over geologic time.

Secondary NRM can result from chemical changes affecting ferromagnetic minerals, exposure to nearby lightning strikes, or long-term exposure to the geomagnetic field subsequent to rock formation. Processes of acquisition of secondary NRM must be examined to understand (1) coexistence of primary and secondary NRM in the same rock, (2) how multiple components of NRM can be recognized, and (3) how partial demagnetization procedures can preferentially erase secondary NRM, allowing isolation of primary NRM. Understanding the physics and chemistry of NRM acquisition is a prerequisite to understanding the fidelity and accuracy of primary NRM and the paleomagnetic techniques for its determination.

THERMOREMANENT MAGNETISM (TRM)

Thermoremanent magnetism (TRM) is NRM produced by cooling from above the Curie temperature (T_c) in the presence of a magnetic field. TRM is the form of remanent magnetism acquired by most igneous rocks. From the previous section, it is understood that magnetic moments of ferromagnetic grains will be stable to time decay at or below the respective blocking temperatures, T_B, which are distributed downward from the Curie temperature. As temperature decreases through T_B of an individual SD grain, that grain experiences a dramatic increase in relaxation time, τ, and changes behavior from superparamagnetic to stable single domain. It is the action of the magnetic field at the blocking temperature that produces TRM.

A significant aspect of TRM is that a small magnetic field (e.g., the surface geomagnetic field) can, at elevated temperatures, impart a small bias in the distribution of magnetic moments of the ferromagnetic grains during cooling and produce a remanent magnetization. At surface temperatures, this remanence can be stable over geologic time and resistant to effects of magnetic fields after original cooling.

A theoretical model

Here we examine a theoretical model for acquisition of TRM. The model is essentially that of French physicist Louis Néel and explains acquisition of TRM by an assemblage of single-domain ferromagnetic grains.

In this model, depicted schematically in Figure 3.9, we consider an assemblage of identical SD grains. The assemblage is assumed to have *uniaxial anisotropy*, meaning that magnetic moments of the grains can point only along some arbitrary axis, but in either direction; above T_B, they will flip rapidly between these two antiparallel directions. One could actually make such an assemblage of SD grains by distributing highly elongated SD magnetite grains in a diamagnetic matrix with long axes of the magnetite grains perfectly aligned.

Now consider a magnetic field applied along the axes of the grains. There is an interaction energy between the applied magnetic field, ***H***, and the magnetic moment, ***m***, of each SD grain (Equation (1.4)):

$$E = -\mathbf{m} \cdot \mathbf{H} \tag{3.18}$$

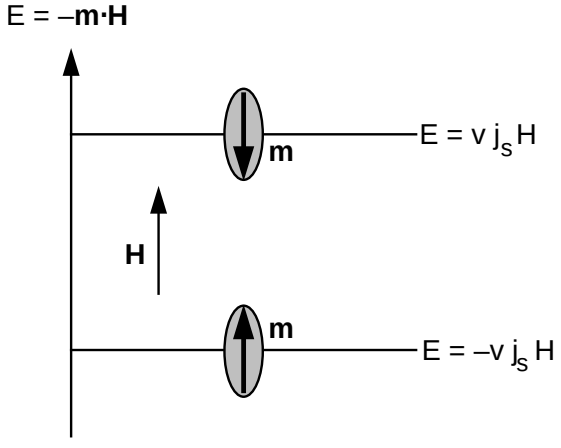

Figure 3.9 Model for TRM acquisition. SD ferromagnetic grains have uniaxial anisotropy, so magnetic moments ***m*** of SD grains are parallel or antiparallel to applied magnetic field ***H***; energies of interaction E_H between magnetic moments of SD grains and the applied magnetic field are shown for the parallel and antiparallel states; v is the SD grain volume; j_S is the saturation magnetization of ferromagnetic material.

Figure 3.9 shows the two possible orientations of magnetic moments of the SD grains and the attendant interaction energy. For grains with ***m*** parallel to ***H***,

$$E = -mH = -v\, j_s H \tag{3.19}$$

where v is the volume of the SD grain and j_s is the saturation magnetization. For grains with ***m*** antiparallel to ***H***,

$$E = mH = v\, j_s H \tag{3.20}$$

The energy difference between these two states results in a preference for occupying the state with ***m*** parallel to ***H***. However, this aligning influence is countered by the randomizing influence of thermal energy, which, in the absence of a magnetizing field, will equalize the population of the two states, thereby yielding no net magnetization.

Above the blocking temperature, magnetic moments of these SD grains will flip rapidly between the parallel and antiparallel states. But because of aligning energy of the applied magnetic field, magnetic moments of individual grains will spend slightly more time in the parallel than the antiparallel state. Collectively, the assemblage will have more grains in the parallel state than in the antiparallel state. A bias of magnetic moments parallel to the applied magnetic field results.

The degree of alignment at the blocking temperature is of major importance. If the magnetic field were switched off at $T > T_B$, the population of the two stable states would quickly equalize, yielding no net magnetization. At or above T_B, the degree of alignment depend upon the ratio of aligning energy to thermal energy. At T_B, this ratio is given by

$$\left(\frac{v\, j_s[T_B]\, H}{\mathrm{k}T_B}\right) = b \tag{3.21}$$

From statistical thermodynamics, the relative Boltzmann probability, P_+, of a grain occupying the energy state with ***m*** parallel to ***H*** is given by

$$P_+ = \left(\frac{\exp[b]}{\exp[b] + \exp[-b]}\right) \tag{3.22}$$

The relative probability, P_-, of the grain occupying the antiparallel state is given by

$$P_- = \left(\frac{\exp[-b]}{\exp[b] + \exp[-b]}\right) \tag{3.23}$$

The bias of magnetic moments (degree of alignment) along H is then

$$P_+ - P_- = \left(\frac{\exp[b] - \exp[-b]}{\exp[b] + \exp[-b]}\right) = \tanh(b) \tag{3.24}$$

This bias of magnetic moments will be frozen (blocked) as the assemblage cools through T_B.

At the blocking temperature, the thermoremanent magnetization will be given by

$$\mathrm{TRM}(T_B) = \left[N(T_B)\; m(T_B)\right]\left[P_+ - P_-\right] \tag{3.25}$$

where $N(T_B)$ is the number of SD grains per unit volume with blocking temperature T_B and $m(T_B)$ is the magnetic moment of an individual SD grain. Inserting $m(T_B) = v\, j_s(T_B)$ and Equation (3.24) for $P_+ - P_-$ yields a complete expression for TRM at the blocking temperature:

$$\mathrm{TRM}(T_B) = N(T_B)\; v\, j_s(T_B)\; \tanh\left(\frac{v\, j_s[T_B]\, H}{\mathrm{k}\, T_B}\right) \tag{3.26}$$

To emphasize that the degree of alignment is small, consider the expected degree of alignment of magnetic moments for an assemblage of SD magnetite grains with blocking temperature of 550°C (= 823°K). The hyperbolic tangent term in Equation (3.26) indicates the degree of alignment and the terms required are v = SD grain volume; T_B = blocking temperature (= 823°K); H = magnetizing field (we'll use 1 Oe); and $j_s(T_B)$ = saturation magnetization at T_B. To illustrate changes in relaxation time with temperature (Figure 3.8), we previously considered SD magnetite particles with T_B = 550°C. The volume of these particles is 4.3×10^{-17} cm^3 and j_s at 550°C = 140 G. The argument of the hyperbolic tangent in Equation (3.26) becomes

$$\left(\frac{v\, j_s[T_B]\, H}{\mathrm{k}\, T_B} \right) = 5.3 \times 10^{-2} \tag{3.27}$$

For such small arguments, tanh $x \approx x$, so the degree of alignment = 0.053. This is indeed a small bias; only a tiny fraction more magnetic moments are aligned with the magnetic field than against it.

With the assumption of a sharp blocking temperature, no further changes in orientations of magnetic moments occur during cooling to ambient surface temperature (ca. 20°C). The only quantity which changes during cooling from T_B to 20°C is saturation magnetization of the ferromagnetic material. Thus the final TRM at 20°C is given by

$$TRM(20^\circ\mathrm{C}) = N(T_B)\; v\, j_s(20^\circ\mathrm{C})\; \tanh\left(\frac{v\, j_s[T_B]\, H}{\mathrm{k}\, T_B} \right) \tag{3.28}$$

Notice that the hyperbolic tangent term of this equation for TRM does not change upon cooling from TB to 20°C because that term is the bias ($P_+ - P_-$) at T_B, which will not change during subsequent cooling. As shown in a previous section, relaxation time, τ, does continue to increase dramatically during cooling below T_B. The resulting TRM can have a relaxation time exceeding geologic time and can thus be stable against time decay.

This simple model illustrates essential features of TRM. It shows how a modest magnetizing field can impart a TRM during cooling through the blocking temperature and how that TRM can be retained over geological time.

Generalizing the model

There are several inadequacies in the above model. The most severe assumption is that the assemblage of SD grains has uniaxial anisotropy. This assumption provides useful simplifications in the mathematical development, but of course it is not realistic. What we expect to encounter in a rock is an assemblage of ferromagnetic grains with essentially random (isotropic) distribution of easy axes of magnetization.

A random distribution of easy axes can be dealt with by setting aligning energy for a particular grain equal to

$$E = \mathbf{m} \cdot \mathbf{H} = mH \cos\theta \tag{3.29}$$

where θ is the angle between the easy axis of magnetization and ***H***. Integration over an isotropic distribution of grains yields a TRM expression that is slightly more complicated than Equation (3.28). However, the essence of the physics is the same.

For an assemblage of SD grains with random distribution of easy axes, the resulting medium is isotropic for acquisition of TRM. This means that TRM will be parallel to the magnetizing field present during cooling. Although not unknown, igneous rocks with significant anisotropy are rare, and we expect that TRM of most igneous rocks will faithfully record the direction of the magnetic field during cooling.

The model just presented also assumes that all SD grains are identical, with only a single blocking temperature. Real rocks have a distribution of sizes and shapes of ferromagnetic grains and consequently have a distribution of T_B. With distributed blocking temperatures, TRM acquisition can be visualized by using the v–h_c diagrams of Figure 3.10. Just below the Curie temperature, microscopic coercive force, h_c, is low, and all grains are superparamagnetic (Figure 3.10a). During cooling, h_c of all grains increases, and

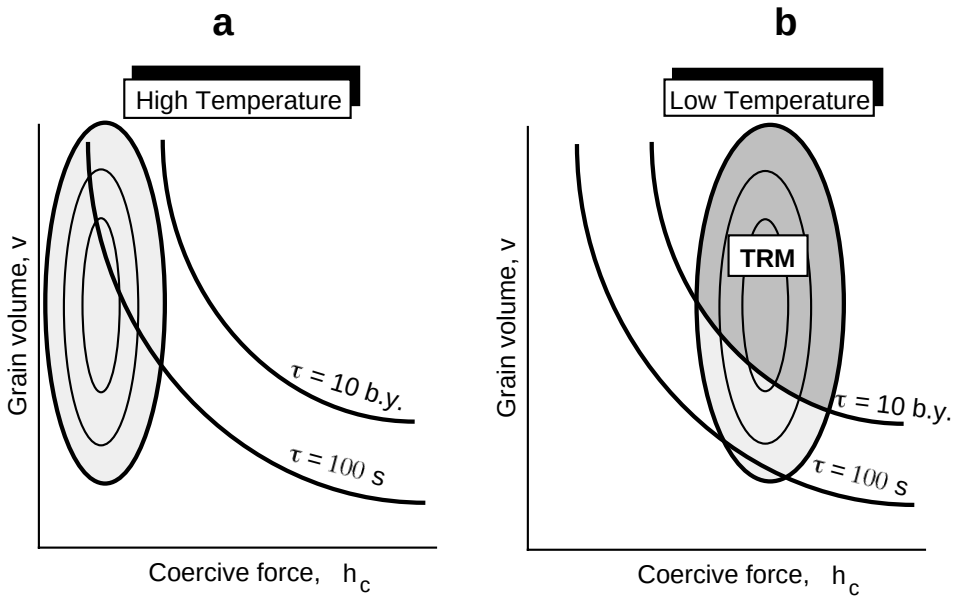

Figure 3.10 Migration of SD grain population towards increasing h_c between (**a**) high temperature and (**b**) low temperature. Lines of τ = 100 s and τ = 10 b.y. are schematically shown; SD grains in the dark stippled region of (**b**) experience blocking of their magnetic moment during cooling and acquire TRM.

the distribution of grains migrates toward increasing h_c (Figure 3.10b). At the respective blocking temperatures, grains pass through the $\tau = \tau_s$ line, change from superparamagnetic to stable SD, and acquire TRM.

The exact distribution of TB depends on the distribution of grain sizes and shapes in the rock and is routinely determined in the course of thermal demagnetization. This process erases remanent magnetization in all grains with blocking temperatures up to the maximum temperature of the laboratory heating. By this technique it is possible to determine the portion of TRM that is blocked within successive T_B intervals. A typical example is shown in Figure 3.11.

Igneous rocks with stable TRM commonly have T_B within about 100°C of the Curie temperature. Rocks with a large portion of remanent magnetization carried by grains with T_B distributed far below T_c are more likely to have complex, multiple-component magnetizations. These difficulties are explored later.

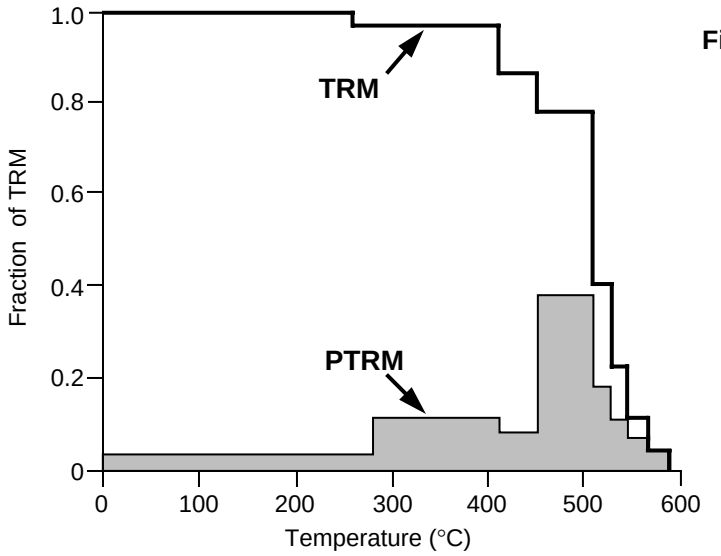

Figure 3.11 Distribution of blocking temperatures in an Eocene basalt sample. The solid line labeled TRM indicates the amount of TRM remaining after step heating to increasingly higher temperature (~75% of the original TRM has blocking temperatures between 500°C and 580°C); the stippled histogram labeled PTRM shows the amount of TRM within corresponding intervals of blocking temperature (e.g., ~40% of the original TRM has a blocking temperatures between 450°C and 510°C).

PTRM

The total TRM can be broken into portions acquired in distinct temperature intervals. For example, TRM of an igneous rock containing magnetite as the dominant ferromagnetic mineral can be broken into portions acquired within windows of blocking temperatures from T_c = 580°C down to 20°C. The portion of TRM blocked in any particular T_B window is referred to as "partial TRM," often abbreviated PTRM. Each PTRM is a vector quantity, and **TRM** is the vector sum of the **PTRM**s contributed by all blocking temperature windows:

$$\mathbf{TRM} = \sum_n \mathbf{PTRM}(T_{Bn}) \tag{3.30}$$

Individual **PTRM**s depend only on the magnetic field during cooling through their respective T_B intervals and are not affected by magnetic fields applied during cooling through lower temperature intervals. This is the *law of additivity of **PTRM**.*

As an example of additivity of **PTRM**, again consider an igneous rock with magnetite as the dominant ferromagnetic mineral. The rock originally cooled to produce a **TRM** that is the vector sum of all **PTRM**s with T_B distributed from T_c to room temperature. If the magnetic field was constant during the original cooling, all **PTRM**s are in the same direction. Now consider that this rock is subsequently reheated for even a short time to a temperature, T_r, intermediate between room temperature and the Curie temperature and then cooled in a different magnetizing field. All **PTRM**s with $T_B < T_r$ will record the new magnetic field direction. However, neglecting time-temperature effects to be considered later, the **PTRM**s with $T_B > T_r$ will retain the **TRM** record of the original magnetizing field. This ability to strip away components of magnetization held by grains with low T_B while leaving the higher T_B grains unaffected is a fundamental element of the thermal demagnetization technique.

Grain-size effects

Perhaps the most severe simplification in the above model of TRM acquisition is that it considers only single-domain grains. Given the restricted range of grain size and shape distributions for stable SD grains of magnetite or titanomagnetite, only a small percentage of grains in a typical igneous rock are truly SD. Most grains are PSD or MD. The question then arises as to whether PSD and MD grains can acquire TRM.

Figure 3.12 shows the particle size dependence of TRM acquired by magnetite in a magnetizing field of 1 Oe (0.1 mT). Note that Figure 3.12 is a log-log plot and efficiency of TRM acquisition drops off dramatically in the PSD grain-size range from 1 μm to about 10 μm. However, PSD grains do acquire TRM that can be stable against time decay and against demagnetization by later magnetic fields. The physics of PSD grains is much more complicated than for SD grains and is not fully understood. However, the basic idea of acquiring TRM by imparting a bias in directions of magnetic moments of PSD grains at the blocking temperature also applies to these inhomogeneously magnetized grains.

For grains of $d > 10$ μm, the acquisition of TRM is inefficient. In addition, acquired TRM in these larger grains generally decays rapidly with time, and these grains are prone to acquire viscous magnetization (discussed below). SD and PSD grains are the effective carriers of TRM, while larger MD grains are likely to carry a component of magnetization acquired long after original cooling.

It has been observed that grain-size distributions of ferromagnetic grains in igneous rocks tend to be *log normally distributed*. A histogram of number of grains versus logarithm of the grain dimension is reasonably fit by a Gaussian (bell-shaped) curve. Rapidly cooled volcanic rocks generally have grain-size distributions peaking at $d < 10$ μm, with a major portion of the distribution within SD and PSD ranges. Also deuteric oxidation of volcanic rocks often produces intergrowth grains with effective magnetic grain size less than the FeTi-oxide grains that crystallized from the igneous melt. Thus, volcanic rocks are commonly observed to possess fairly strong and stable TRM. A typical intensity of TRM in a basalt flow is 10^{-3} G (1 A/m). Generally, a smaller percentage of the grain-size distribution in volcanic rocks than in intrusive igneous rocks is

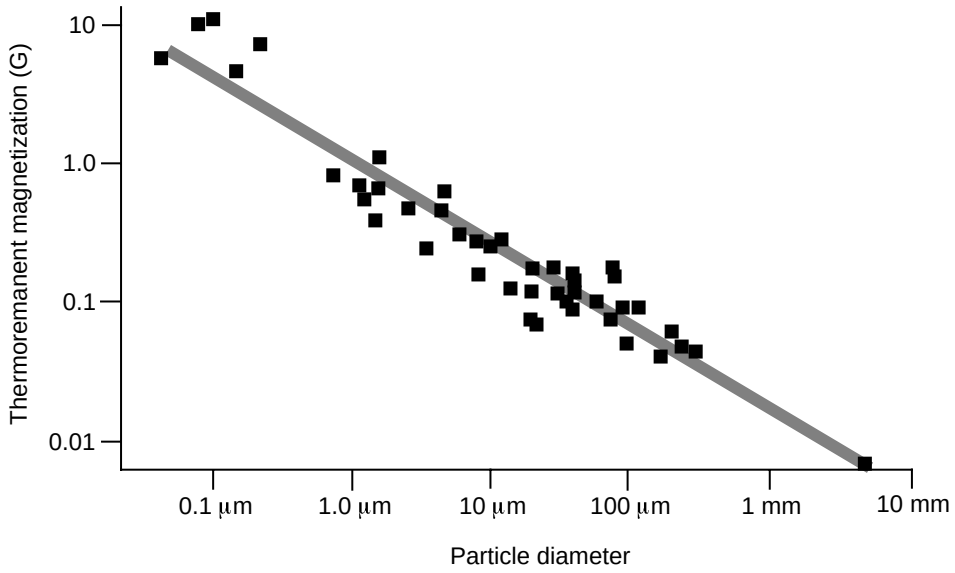

Figure 3.12 Dependence of intensity of TRM on particle diameter of magnetite. Magnetite particles were dispersed in a matrix; the intensity of TRM is determined per unit volume of magnetite to allow comparison between experiments that used varying concentrations of dispersed magnetite; the magnetizing field was 1 Oe. Redrawn after Dunlop (*Phys. Earth Planet. Int.*, v. 26, 1–26, 1981).

within the MD range. This means that secondary components of magnetization carried by MD grains are minimized in volcanic rocks.

However, for intrusive igneous rocks the opposite situation prevails. Grain-size distribution peaks at larger sizes, and a majority of the grains are within the MD range with only a small percentage within SD and PSD ranges. Accordingly, the intensity of the stable TRM component (if present at all) is diminished in comparison to volcanic rocks. More important, secondary components of magnetization carried by MD grains can dominate the magnetization. Removing this noise component to reveal the underlying stable TRM component can be a major challenge.

Mafic intrusive rocks are more likely to retain a primary TRM than are felsic intrusives. Mafic intrusives have higher Fe and Ti contents with the result that intermediate composition titanomagnetite grains often undergo exsolution during cooling. These exsolved grains are much more capable of carrying stable TRM than are homogeneous grains. In addition, many intrusive rocks containing a stable TRM component are found to contain SD magnetite grains exsolved in host plagioclase or other silicate grains (Figure 2.11a). From this discussion, it is clear that volcanic rocks are much preferred over intrusive rocks in paleomagnetic studies.

CHEMICAL REMANENT MAGNETISM (CRM)

Chemical changes that form ferromagnetic minerals below their blocking temperatures in a magnetizing field result in acquisition of *chemical remanent magnetism* (CRM). Chemical reactions involving ferromagnetic minerals include (a) alteration of a preexisting mineral (possibly also ferromagnetic) to a ferromagnetic mineral or (b) precipitation of a ferromagnetic mineral from solution. Although exceptions exist, CRM is most often encountered in sedimentary rocks. This section outlines a model of CRM acquisition that explains the basic attributes of this type of NRM.

Model of CRM formation

As in the development of a model for thermoremanent magnetism (TRM), we start with Equation (3.14) describing relaxation time, τ, of an assemblage of identical single-domain (SD) grains:

$$\tau = \left(\frac{1}{\mathrm{C}}\right)\exp\left(\frac{v\, h_c\, j_s}{2\mathrm{k}T}\right) \tag{3.14}$$

During TRM formation, volume (v) of the SD grains is constant, but τ increases during cooling because h_c and j_s increase as T decreases. During formation of chemical remanent magnetism, temperature is constant (usually ambient surface temperature). Accordingly, j_s and h_c are approximately constant. During chemical formation of a ferromagnetic mineral, individual grains grow from zero initial volume. Grains with small volumes have short relaxation times and are superparamagnetic. This is depicted in Figure 3.13a, with distribution of SD grains in v–h_c space compressed toward the abscissa. As growth of the ferromagnetic grains proceeds, volume of individual grains increases, and the distribution in v–h_c space migrates upward (Figure 3.13b). During grain growth, individual grains experience dramatic increase in relaxation time and change from superparamagnetic to stable single domain. The grain volume at which this transition occurs is referred to as the *blocking volume*. As assemblages of grains pass through the blocking volume, a bias of magnetic moments toward the applied magnetic field is recorded, just as with TRM. Continued grain growth following blocking of CRM can produce a chemical remanent magnetization that is stable over geological time.

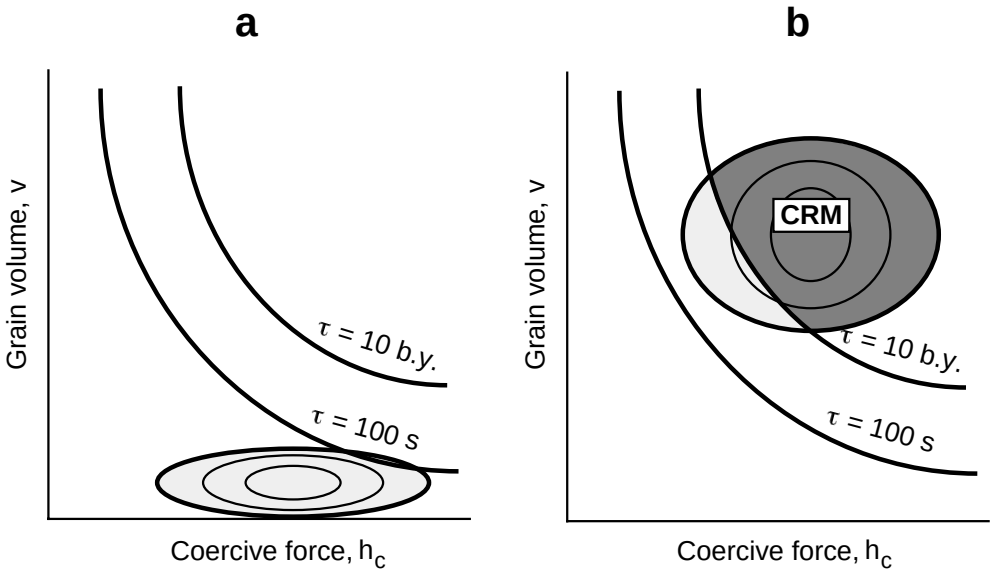

Figure 3.13 Migration of SD grain population toward increasing grain volume, v, between (**a**) beginning of chemical precipitation and (**b**) an advanced stage of grain precipitation. Lines of τ = 100 s and τ = 10 b.y. are schematically shown; SD grains in the dark stippled region of (**b**) have grown through blocking volumes and have acquired CRM.

Laboratory experiments on synthetic CRM have verified the essential elements of this model. Experiments involving precipitation of ferromagnetic minerals from solution show that CRM accurately records the direction of the magnetic field. Experiments involving alteration of one ferromagnetic mineral to another also have been performed. When the alteration involves a major change of crystal structure (e.g., magnetite to hematite), acquired CRM records the magnetic field direction during alteration and does not seem to be affected by the magnetization of the preexisting ferromagnetic mineral. However, when alteration occurs with no fundamental change of crystal structure (e.g., titanomagnetite to titanomaghemite), the resulting remanence can be controlled by the remanence direction of the original grains.

An example of natural CRM is postdepositional formation of hematite, primarily in red sediments. A typical intensity of CRM in a red siltstone is 10^{-5} G (10^{-2} A/m). A variety of postdepositional oxidation and

dehydration reactions play a role in formation of hematite. For example, goethite (αFeOOH) is an oxyhydroxide produced by alteration of Fe-bearing silicates. Goethite can dehydrate to hematite by the following reaction:

$$2\ (\alpha\text{FeOOH}) \rightarrow \alpha\text{Fe}_2\text{O}_3 + \text{H}_2\text{O}\ (\text{evaporates}) \tag{3.31}$$

CRM is acquired during growth of the resulting hematite grains.

When hematite is produced soon after deposition, the CRM will record the magnetic field direction essentially contemporaneous with deposition and is regarded as a primary magnetization. However, the mode and timing of acquisition of remanent magnetism in red sediments are a matter of controversy. Because red sediments have been a major source of paleomagnetic data, appreciation of the processes involved in magnetization of red sediments (and attendant uncertainties) is important. Accordingly, we will discuss this red bed controversy in Chapter 8.

CRM may be regarded as a secondary component if it is acquired long after deposition. For example, diagenetic/authigenetic formation of Fe-sulfides and MnFe-oxides in marine sediments can lead to formation of CRM. This CRM may be acquired millions of years after deposition and would be regarded as a secondary magnetization. These topics are also discussed in Chapter 8.

DETRITAL REMANENT MAGNETISM (DRM)

Detrital remanent magnetism (DRM) is acquired during deposition and lithification of sedimentary rocks. In most sedimentary environments, the dominant detrital ferromagnetic mineral is magnetite (or Ti-poor titanomagnetite). DRM is complicated because many complex processes can be involved in the formation of sedimentary rocks. There is a wide variety of initial mineralogies, and constituent minerals often are not in chemical equilibrium with each other or with the environment of deposition. Postdepositional physical processes such as bioturbation can affect magnetization. Compaction is a particularly important postdepositional process and will be a topic of special consideration in Chapter 8. Chemical processes can also alter or remove original detrital ferromagnetic minerals and/or precipitate new ferromagnetic minerals, with attendant effects on the paleomagnetic record. Because of these complexities, DRM is less well understood than is TRM, and there are more uncertainties about the accuracy of paleomagnetic recordings in sedimentary rocks.

In this section, basic physical and chemical processes affecting paleomagnetism of sedimentary rocks are outlined. We start with physical alignment occurring at the time of deposition and refer to the resulting remanence as *depositional detrital remanent magnetism*. We then discuss physical alignment processes, termed *postdepositional detrital remanent magnetism* (pDRM), that occur after deposition but before consolidation. pDRM processes can operate in the upper 10–20 cm of the accumulating sediment, where water contents are high. The combination of depositional and postdepositional magnetization processes is referred to as detrital remanent magnetism (DRM).

Depositional DRM (the classic model)

The classic model for acquisition of DRM considers only the aligning influence of a magnetic field on a ferromagnetic particle at the moment it encounters the sediment/water interface. We consider a spherical ferromagnetic grain with magnetic moment, $\boldsymbol{m}$, immersed in fluid of viscosity, η, and acted upon by magnetic field, $\boldsymbol{H}$. The angle between $\boldsymbol{m}$ and $\boldsymbol{H}$ is θ (Figure 3.14). The equation of motion which describes the alignment is

$$\Omega\left(\frac{d^2\theta}{dt^2}\right) + \beta\left(\frac{d\theta}{dt}\right) + mH\sin\theta = 0 \tag{3.32}$$

The first term describes inertial resistance to angular acceleration. Ω is moment of inertia of the particle given by

$$\Omega = \left(\frac{\pi\, d^5 \rho}{60}\right) \tag{3.33}$$

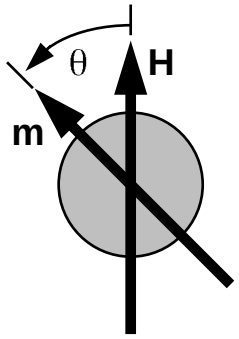

Figure 3.14 Detrital ferromagnetic grain in magnetic field. ***m*** is the magnetic moment of the ferromagnetic grain; ***H*** is magnetic field; θ is angle of ***m*** from ***H***; resulting aligning torque is $\boldsymbol{\Gamma} = \boldsymbol{m} \times \boldsymbol{H}$.

where ρ is the density of the particle and d is the grain diameter. The second term in Equation (3.32) describes viscous drag between the particle and surrounding fluid. This drag resists rotation of the particle and depends upon rotation rate with β given by

$$\beta = \pi d^3 \eta \tag{3.34}$$

The last term in Equation (3.32) is the aligning torque of the magnetic field.

For values appropriate to ferromagnetic particles in sedimentary rocks, the inertial term (first term in Equation (3.32)) is negligible. This means that the grain rotates quickly and approaches small values of θ for which $\sin \theta \approx \theta$. The resulting simplifications to Equation (3.32) yield the following governing equation:

$$\frac{d\theta}{dt} = -\left(\frac{mH\theta}{\pi d^3 \eta} \right) \tag{3.35}$$

The solution to this equation will describe how the angle θ will decrease from an initial angle θ_0. The solution describing this alignment process is

$$\theta(t) = \theta_0 \exp\left(\frac{-t}{t_0} \right) \tag{3.36}$$

where

$$t_0 = \left(\frac{\pi d^3 \eta}{mH} \right) \tag{3.37}$$

So this is an exponential alignment process in which t_0 is a characteristic alignment time during which θ decreases from θ_0 to θ_0 / e.

Now we proceed by realizing that the magnetic moment of the spherical particle is simply

$$m = \frac{\pi d^3 j}{6} \tag{3.38}$$

where j is the net magnetic moment per unit volume. Substituting this expression for m back into Equation (3.37) yields t_0, the characteristic alignment time:

$$t_0 = \frac{6\eta}{jH} \tag{3.39}$$

This result shows that t_0 is independent of particle size, d.

To gain a feeling for the magnitude of t_0, substitute the following values into Equation (3.39):

η = 10^{-2} poise, appropriate value for water
H = 0.5 Oe, typical surface geomagnetic field
j = 0.1 G

The latter value is appropriate for a large PSD grain of magnetite but is much lower than expected for a small PSD grain or an SD grain. However, even using this modest value for j, we find that Equation (3.39) yields t_0 = 1 s. The model implies rapid (and complete) alignment of ferromagnetic particles with the geomagnetic field at the time of deposition. Unfortunately, this theory fails a number of reality checks.

Evidence for postdepositional alignment

Laboratory redeposition experiments provide insight into DRM processes. In a number of experiments, natural sediments have been dispersed in water, then redeposited under known laboratory conditions. Results of such experiments are significantly different than predicted by the classic model.

One of the earliest laboratory redeposition experiments involved Holocene glacial varved deposits. The degree of alignment of magnetic moments (determined from resulting DRM) was found to be far less than implied by the classic model. Apparently, some (randomizing?) agent prevents the predicted high degree of alignment.

Redeposition experiments have been performed with inclination of the magnetizing field varied from one experiment to the next. Results are shown in Figure 3.15a. Inclination of the resulting DRM, I_0, was found to be systematically shallower than inclination of the applied magnetic field, I_H, to which it was related by

$$\tan I_0 = f \tan I_H \tag{3.40}$$

The value of f in Equation (3.40) is 0.4 for redeposited glacial sediments.

One can visualize a simple explanation for this observation by examining the schematic diagram of Figure 3.15b. Because of shape anisotropy, the magnetic moment of elongated ferromagnetic grains lies along the long axis of the particle. But gravitational torques cause such particles to rotate toward the horizontal. However, in natural sediments, *inclination error* tends to be less than expected from these redeposition experiments and is often absent. The general conclusion is that the magnetization process must be in part a postdepositional detrital remanent magnetization (pDRM). Inclination error is more completely discussed in Chapter 8.

Results of an experiment that clearly demonstrated the feasibility of pDRM are shown in Figure 3.16. Dry mixtures of magnetite and quartz were made, then exposed to a magnetizing field while flooded with water and subsequently dried. Resulting pDRM was found to accurately record the inclination of the applied field. Ferromagnetic particles were able to reorient in the water-rich slurry, leading to accurate recording of the applied magnetic field direction.

Another enlightening experiment involved redeposition of deep-sea sediments (Figure 3.17). Over a number of days, sedimentary layers were redeposited under controlled magnetic field conditions. The declination of the applied magnetic field was switched by 180° on day 62. Whereas the change in declination of the applied magnetic field was essentially instantaneous, the resulting declination change in the sediment column was spread out, showing a time-integrative effect and a time lag in the magnetization process. Most significantly, the change in declination was partially recorded by sediments deposited 10 or 20 days before the change in direction of the applied magnetic field.

Natural deep-sea sediments are generally bioturbated to depths of 20 cm or more. It seems certain that any depositional DRM will be wiped out by passage of sediment through the digestive tract of a worm (if not on the intake, then certainly on the outgo). Yet bioturbated deep-sea sediments often are accurate recorders of the magnetic field present shortly after deposition. All of these laboratory experiments and natural processes emphasize the importance of postdepositional DRM. In many sediment types such as bioturbated sediments, pDRM is the only plausible mechanism for acquisition of DRM. Other sediments possess a resultant magnetization that is probably a combination of depositional and postdepositional alignment. An analysis of the pDRM process is essential to understanding detrital remanent magnetism.

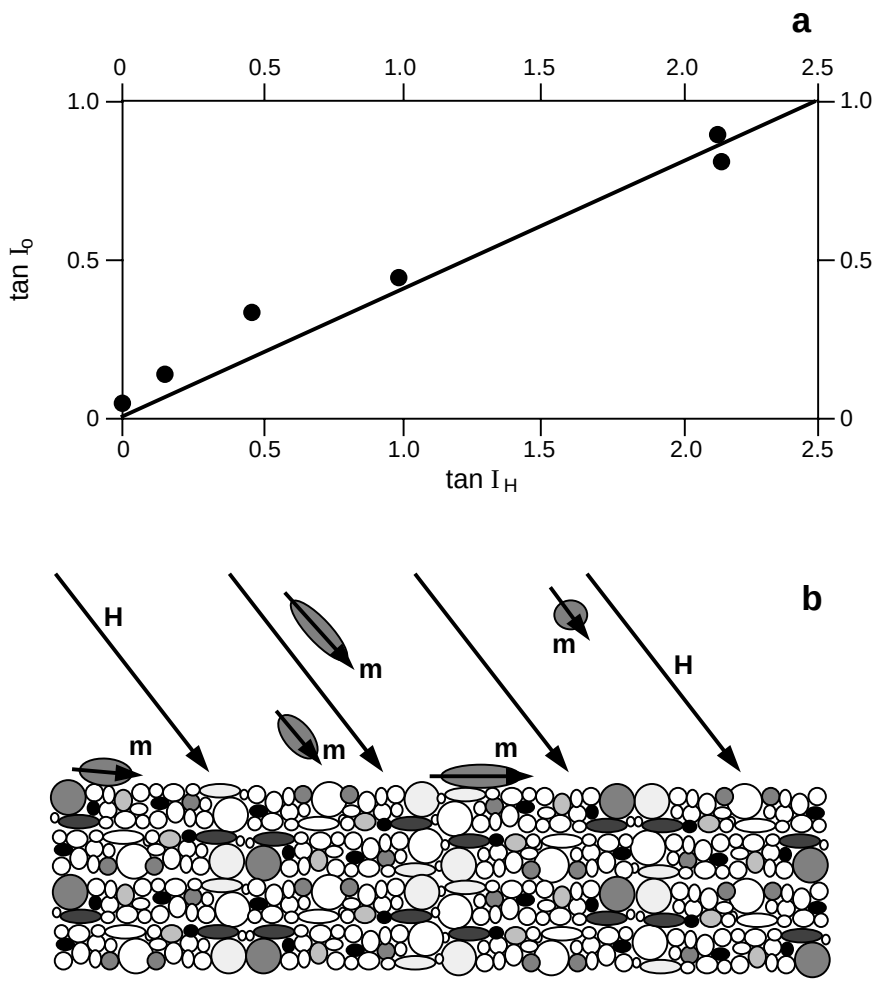

Figure 3.15 (**a**) The relationship between inclination (I_0) of DRM in redeposited glacial sediment and the inclination of the applied magnetic field (I_H). The solid line is the graph of tan I_0 = 0.4 tan I_H. Redrawn from Verosub (1977). (**b**) Schematic representation of ferromagnetic grains with magnetic moments ***m*** settling in magnetic field ***H***. Elongate grains with ***m*** along long axis tend to rotate toward the horizontal plane, resulting in shallowed inclination of DRM.

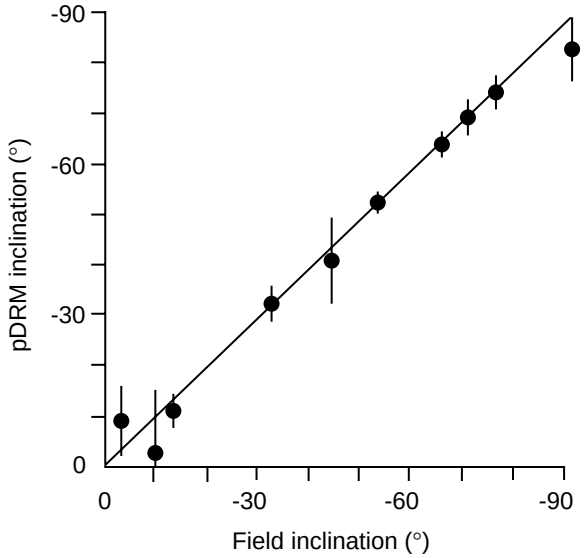

Figure 3.16 Inclination of pDRM versus inclination of applied magnetic field. Samples were dry synthetic quartz-magnetite mixtures flooded with water in a magnetic field of varying inclination; vertical error bars are confidence limits on measured pDRM inclination; the solid line is the expected result for perfect agreement between inclinations of pDRM and the applied magnetic field. Redrawn from Verosub (1977).

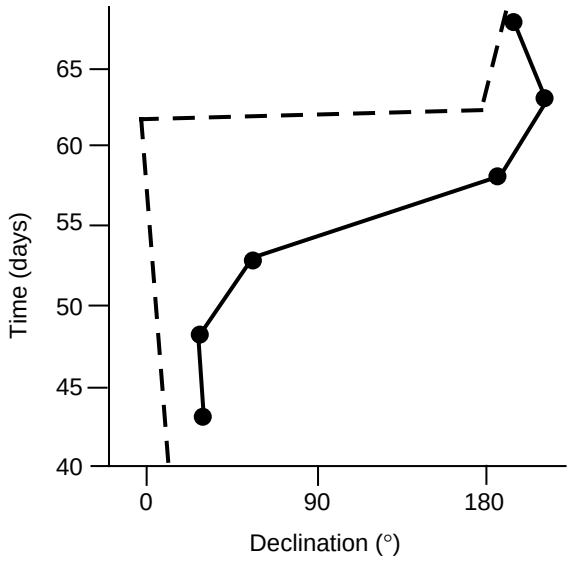

Figure 3.17 Declination of DRM recorded by redeposited deep-sea clay compared with declination of an applied magnetic field during redeposition. The ordinate indicates the number of days since commencement of the redeposition experiment; the declination of the applied magnetic field was changed by 180° on day 62; sediment deposited at least 10 days before the change in magnetic field declination partially recorded the new magnetic field direction. Redrawn from Verosub (1977).

Brownian motion and postdepositional alignment

As with thermoremanent magnetism, an important randomizing influence in DRM is thermal energy. In the postdepositional environment, thermal energy is transmitted to ferromagnetic particles by jostling from *Brownian motion* of water molecules. It is quite likely that the amount of misalignment depends on particle size; submicron particles are more severely jostled by water molecules than are 100-μm particles. Early attempts to develop a theory of pDRM likened the physical rotation of small ferromagnetic grains within water-filled pore spaces to alignment of atomic magnetic moments in a paramagnetic gas. In both situations there is an aligning torque of the magnetic field opposed by a randomizing influence of thermal energy.

First consider an assemblage of identical ferromagnetic particles with magnetic moment ***m***. As with paramagnetism, the Langevin theory is applicable and leads to

$$\frac{\text{pDRM}}{\text{pDRM}_\text{s}} = \coth\left(\frac{mH}{\text{k}T}\right) - \left(\frac{\text{k}T}{mH}\right) \tag{3.41}$$

where pDRM is the resulting pDRM and pDRM_s is the saturation pDRM, the remanent magnetism that would result if all magnetic moments were rigidly aligned.

The *Brownian motion theory of pDRM* has been refined by considering grain magnetic moments to be distributed over a range from 0 to a maximum value, m_{max}. If the distribution of magnetic moments is uniform between these limits, integration of the above expression over the range of m yields

$$\frac{\text{pDRM}}{\text{pDRM}_\text{s}} = \left(\frac{1}{x}\right) \ln\left(\frac{\sinh x}{x}\right) \tag{3.42}$$

where

$$x = \frac{m_\text{max} H}{\text{k}T} \tag{3.43}$$

This expression is plotted in Figure 3.18a. For small magnetic fields and small particle magnetic moments, the value of x in Equations (3.42) and (3.43) is small. This leads to the approximation

$$\frac{\text{pDRM}}{\text{pDRM}_\text{s}} = \frac{x}{6} = \frac{m_\text{max} H}{6\text{k}T} \tag{3.44}$$

This result predicts the initial slope shown in Figure 3.18a.

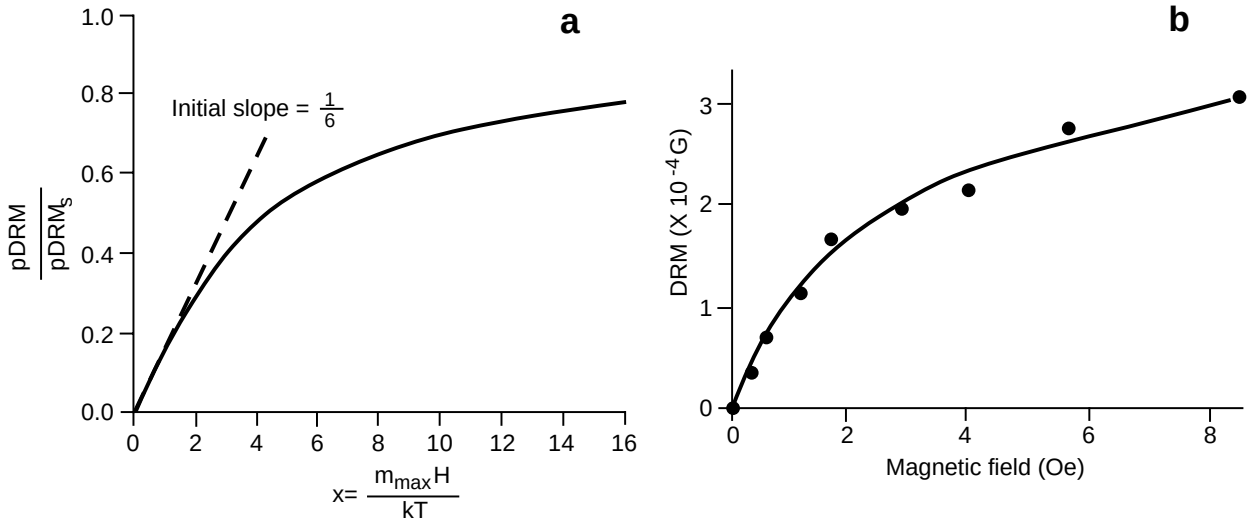

Figure 3.18 (**a**) Theoretical fractional saturation of pDRM in Brownian motion theory. The solid line is a plot of Equation (3.42); for small *x*, slope is 1/6. (**b**) DRM acquired by redeposited glacial varved clay as a function of applied magnetic field. The solid line is Equation (3.42) with parameters adjusted to best fit observed DRM. Redrawn from Verosub (1977).

As with any such derivation, it is worthwhile examining whether the result is physically reasonable. Predicted pDRM for zero magnetizing field (or for $m_{max} = 0$) is quite reasonably zero. With initial application of a magnetizing field, pDRM logically increases in a linear fashion. In strong magnetizing fields, there is an asymptotic behavior, with pDRM approaching an upper limit. This prediction is reasonable because even an infinite magnetizing field could do no more than perfectly align the constituent magnetic moments. Conversely, for any given magnetizing field, increasing temperature is predicted to decrease resulting pDRM, as expected for increased randomizing influence of Brownian motion. So, under first-order intuitive scrutiny, the governing equation for pDRM seems reasonable.

Experimental data on redeposited glacial sediments are shown by data points in Figure 3.18b, wherein Equation (3.42) was fit to the data. The form of Equation (3.42) fits the experimental data quite well, giving confidence that the theory successfully describes dependence of pDRM on field strength. The parameter for the glacial sediments adjusted to fit the form of Equation (3.42) is m_{max}. The resulting value of m_{max} is 7.4×10^{-14} G cm^3 (7.4×10^{17} A m^2). With information about grain size of magnetite particles, it is possible to determine that intensity of magnetization is 8 G for a typical ferromagnetic grain in this sediment. This value is intermediate between the 480 G expected for SD particles and the low intensity (<1 G) expected for MD grains. This result indicates the importance of PSD grains to magnetization of these silts and clays.

The Brownian motion theory of pDRM has been quite successful in describing many properties of postdepositional detrital remanent magnetism. But success of the theory does not mean that all DRM is actually pDRM. In natural sediments, a portion of DRM may be depositional, forming by action of aligning and gravitational torques at the time of deposition. The remainder is the result of postdepositional alignment. Depositional DRM can lead to inclination error, whereas pDRM realignment tends to remove inclination error. The portion of total DRM resulting from depositional alignment as opposed to pDRM processes is thus of major concern.

The ratio of depositional to postdepositional alignment depends upon a number of factors that are imperfectly understood. Some of the most important are the following:

1. *Grain size.* Small grain size enhances Brownian motion of ferromagnetic particles. Fine-grained sediments have high water contents when initially deposited and slowly decrease in water content during initial compaction and consolidation. Accordingly, there is ample time (perhaps 10^2–10^3 yr)

for pDRM alignment to operate. Conversely, coarse-grained sediments may have a larger portion of total DRM formed by depositional processes.

2. *Rate of deposition*. Residence time for a ferromagnetic particle within the zone of high water content depends on rate of deposition. Slow rates probably enhance postdepositional alignment.
3. *Bioturbation*. Sediments stirred by bioturbation acquire all detrital remanence by postdepositional processes. Bioturbation ensures high water content in the top of the accumulating sediment column, and high water content is known to enhance pDRM alignment.

Grain-size effects

A claystone has a maximum grain diameter of 4 μm, and virtually all magnetite particles are within the SD and PSD ranges. However, grain-size demarcation between silt and sand is 62 μm. Fine silts may have a major portion of grains within the PSD range, but almost all magnetite grains in well-sorted coarse silts or sands are MD.

These differences in grain size have dual importance. First, grains within SD or PSD ranges have relatively strong magnetization. These fine particles are more efficiently aligned by the geomagnetic field (dominantly by pDRM). Larger particles have lower intensity of magnetization and are less likely to move freely within pore spaces in newly deposited sediment. Thus, they are not effectively aligned by either depositional or postdepositional processes. Second, larger ferromagnetic particles within the MD grain-size range are more susceptible to acquisition of viscous magnetization. Thus, sandstones are less efficiently magnetized initially, and their remanent magnetization is less stable.

Other effects of grain size are also significant. For any grain size larger than medium sandstone, mechanical energies begin to outweigh aligning influence of the geomagnetic field on ferromagnetic particles. Thus, coarse sands and gravels are not likely to acquire substantial DRM. In addition, coarse sediments are generally permeable and likely to experience chemical changes due to groundwater circulation with probable effects on ferromagnetic minerals. For these reasons, claystones to fine sandstones are usually preferred in paleomagnetic studies, and larger grain-size sediments are avoided.

Lock-in of DRM

The locking-in of detrital remanent magnetism occurs when dewatering and consolidation restrains motion of sedimentary particles. Once physical contact of surrounding grains inhibits motion, DRM is mechanically locked. Lock-in is spread over the time interval of dewatering and consolidation. Estimates of lock-in time range up to 10^3 yr, depending on sedimentary environment. Larger ferromagnetic particles are probably locked before fine particles situated in interstices.

This discussion of DRM has provided a basic understanding of remanent magnetization in detrital sedimentary rocks at or soon after deposition. Considering the variations in source rocks and in depositional and postdepositional processes, it is not surprising that DRM has a wide range of intensities. Magnetite-rich continental deposits can have DRM intensities > 10^{-4} G (10^{-1} A/m), while marine limestones can have DRM intensities < 10^{-7} G (10^{-4} A/m).

VISCOUS REMANENT MAGNETISM (VRM)

Viscous remanent magnetism (VRM) is a remanent magnetization that is gradually acquired during exposure to weak magnetic fields. Natural VRM is a secondary magnetization resulting from action of the geomagnetic field long after formation of the rock. From the paleomagnetic viewpoint, this VRM usually is undesirable noise. In this section, we examine basic properties of viscous magnetization. By understanding the basic physics, we can discover the properties of ferromagnetic grains that are prone to acquisition of VRM. In turn, this will explain demagnetization techniques employed to erase viscous components of magnetization to reveal primary components of paleomagnetic interest. We discuss these demagnetization procedures in Chapter 5.

Acquisition of VRM

Experimental data illustrating acquisition of viscous remanence are shown in Figure 3.19. In this experiment, a synthetic sample with dispersed 2-μm grains of magnetite was placed in a magnetic field of 3.3 Oe (0.33 mT). Resulting VRM was measured periodically during exposure to the magnetic field, and the VRM acquisition experiment was repeated at various temperatures. VRM at a given temperature is acquired according to

$$\text{VRM} = S \log t \tag{3.45}$$

where t is the acquisition time (s), the time over which VRM is acquired, and S is the viscosity coefficient.

From Figure 3.19 it is clear that S increases with temperature. Because of logarithmic growth of VRM with time of exposure, viscous magnetization is dominated by the most recent magnetizing field. Rocks that have large components of VRM are usually observed to have NRM aligned with the present geomagnetic field at the sampling location.

We first consider VRM acquired by single-domain grains. For assemblages of SD particles, acquisition of VRM is essentially the inverse of magnetic relaxation. VRM acquisition involves realignment of magnetic moments of grains with short relaxation time, τ. In Figure 3.20, contours of a hypothetical distribution of SD grains are shown on a v–h_c diagram. If the VRM acquisition experiment has been carried out for a length of time equal to "acquisition time," then all grains with $\tau \leq$ acquisition time (grains shown by the heavy stippled pattern in Figure 3.20) are effectively "unblocked" and can respond to the applied magnetic field. Magnetic moments of these unblocked grains seek an equilibrium distribution with resulting VRM in the direction of the applied magnetic field. As acquisition time increases, the line of τ = acquisition time sweeps through the grain distribution, and VRM increases.

The effect of increased temperature can be understood by realizing that h_c decreases with increased temperature. The distribution of grains in v–h_c space migrates toward decreasing h_c (toward the left in the

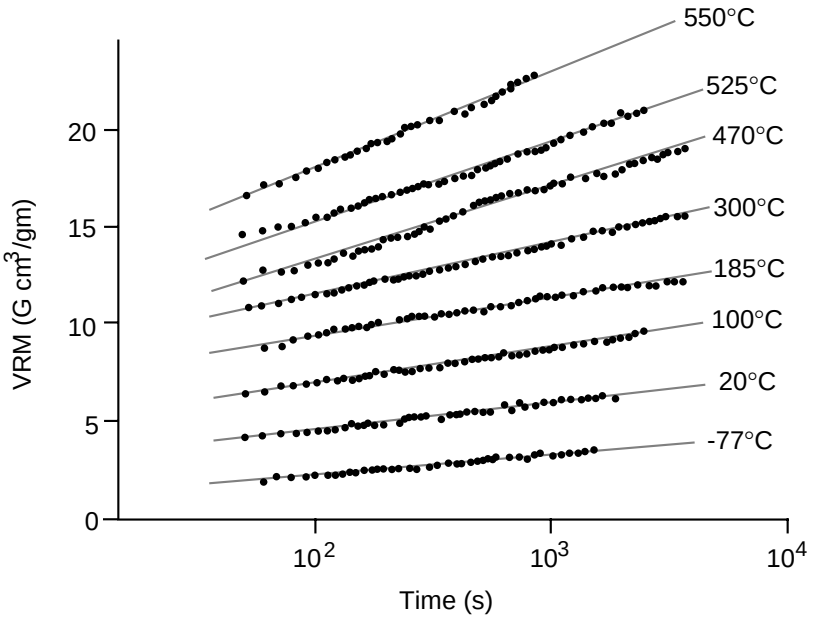

Figure 3.19 Progressive acquisition of VRM by synthetic sample of dispersed 2-mm diameter grains of magnetite. Data points show VRM acquired at corresponding time since the beginning of exposure to the magnetic field; lines show the trend of VRM for a particular VRM acquisition experiment at the temperature indicated; the magnetic field was 3.3 Oe; zero on the ordinate is arbitrary (the absolute value of VRM was adjusted so that results of all VRM acquisition experiments could be conveniently shown on a single drawing). Redrawn from Stacey and Banerjee (1974).

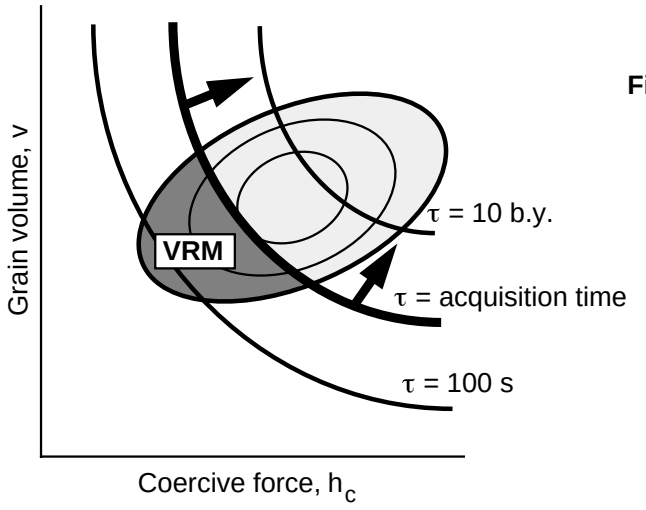

Figure 3.20 Schematic representation of VRM acquisition on a diagram of SD grain volume (v) versus microscopic coercive force (h_c). As the time of VRM acquisition increases, the bold line labeled "τ = acquisition time" sweeps through the SD grain population from lower left to upper right; grains with progressively longer τ can acquire VRM as acquisition time increases; SD grains in the dark stippled region labeled "VRM" have acquired VRM.

v–h_c diagram) as temperature increases. Also more thermal energy means that energy barriers to rotation of the magnetic moment are more quickly overcome. Thus, for a given acquisition time, increasing temperature results in more grains becoming carriers of VRM; hence, viscosity coefficient, S, is increased. For substantially elevated temperature, the resulting VRM is referred to as *thermoviscous remanent magnetization* (TVRM).

In naturally acquired VRM, acquisition time can be up to 10^9 yr or even longer. All grains with $\tau < 10^9$ yr are potential carriers of VRM. SD grains with relaxation times $>10^9$ yr will generally retain primary magnetization of paleomagnetic interest. On the v–h_c diagram, these stable grains with long relaxation time are in the upper right portion of the diagram.

VRM in PSD and MD particles

VRM is acquired by PSD and MD grains through thermal activation of domain walls. As shown in Figure 3.3, domain wall energy is a function of position. Thermal energy can activate domain walls over local energy barriers. Interaction energy between the applied field and the magnetization of the PSD or MD grain favors domain wall motion, resulting in increased magnetization in the direction of the applied field.

For multidomain grains, a general inverse relationship exists between coercive force and viscosity coefficient. Grains of low coercive force rapidly acquire VRM, and grains with the lowest coercive force dominate VRM. For magnetite-bearing rocks, VRM is generally carried by MD grains of low coercive force. This causal connection between low coercivity and dominance of VRM is important in explaining demagnetization of VRM in magnetite-bearing rocks.

Thermoviscous remanent magnetism (TVRM)

Rocks of paleomagnetic interest may suffer intervals of heating, possibly resulting in metamorphism. We must understand how prolonged exposure to elevated temperatures below the Curie temperature will (1) affect the ability of rocks to retain a primary NRM and (2) form thermoviscous magnetization (TVRM). In this section, we present an analysis of TVRM that employs single-domain theory to predict changes in relaxation time with temperature. This theory is quite successful in explaining acquisition of TVRM. It also explains how portions of ferromagnetic particles in rocks can potentially retain a primary paleomagnetic record despite significant metamorphism.

Initially consider an assemblage of identical SD grains. The Néel relaxation time equation with temperature dependences explicitly stated is

$$\tau(T) = \frac{1}{\mathrm{C}} \exp\left(\frac{v j_s[T] h_c[T]}{2\mathrm{k}T} \right) \tag{3.46}$$

which yields

$$\ln(\tau[T]\ \mathrm{C}) = \left(\frac{v\, j_s[T]\, h_c[T]}{2\ \mathrm{k}\ T}\right) \tag{3.47}$$

For an assemblage of identical grains,

$$\frac{v}{2\mathrm{k}} = \text{constant} = \frac{T\ \ln\big(\tau[T]\ \mathrm{C}\big)}{j_s[T]\, h_c[T]} \tag{3.48}$$

Now assume that the assemblage has relaxation times τ_1 at temperature T_1 and τ_2 at temperature T_2. Because the left side of Equation (3.48) is constant, the relationships between parameters at T_1 and T_2 becomes

$$\left(\frac{T_1\ \ln[\tau_1\ \mathrm{C}]}{j_s[T_1]\, h_c[T_1]}\right) = \left(\frac{T_2\ \ln[\tau_2\ \mathrm{C}]}{j_s[T_2]\, h_c[T_2]}\right) \tag{3.49}$$

To predict time-temperature relationships, we must know the temperature dependence of coercive force, $h_c(T)$. For SD magnetite, a reasonable assertion is that coercivity is dominated by shape anisotropy and will be given by

$$h_c(T) = \Delta N_D\ j_s(T) \tag{3.50}$$

where ΔN_D is the difference in internal demagnetizing factor between short and long axes of the SD particle. For SD hematite, coercivity is controlled by magnetocrystalline anisotropy that has more severe temperature dependence given by

$$h_c(T) = D\, {j_s}^3(T) \tag{3.51}$$

where D is a proportionality constant independent of temperature (and depends on all manner of things that are not important to this discussion). Plugging these expressions back into Equation (3.49) yields

$$\left(\frac{T_1\ \ln[\tau_1\ \mathrm{C}]}{{j_s}^2[T_1]}\right) = \left(\frac{T_2\ \ln[\tau_2\ \mathrm{C}]}{{j_s}^2[T_2]}\right) \quad \text{for magnetite;} \tag{3.52}$$

$$\left(\frac{T_1\ \ln[\tau_1\ \mathrm{C}]}{{j_s}4[T_1]}\right) = \left(\frac{T_2\ \ln[\tau_2\ \mathrm{C}]}{{j_s}^4[T_2]}\right) \quad \text{for hematite.} \tag{3.53}$$

Using known temperature dependence of saturation magnetization, js, for magnetite and hematite (Figure 2.3), we can predict time-temperature stabilities.

The most useful way to display the resulting relaxation time and blocking temperature (τ, T_B) pairs is to generate *nomograms* which show the locus of points in τ–T_B space that activate the same grains. Nomograms for SD particles of magnetite and of hematite are shown in Figure 3.21. These diagrams are also known as *blocking diagrams*. An example using Figure 3.21a will reveal the utility of these nomograms.

Point 1 of Figure 3.21a labels a point in τ–T_B space corresponding to SD magnetite grains that have a relaxation time of 10 m.y. at 260°C. These grains are expected to acquire substantial VRM if held at 260°C for 10 m.y. Point 2 corresponds to τ = 30 minutes at T = 400°C and lies on the same nomogram as point 1. This means that grains with τ = 10 m.y. at 260°C also have τ = 30 minutes at 400°C. The implication is that TVRM acquired by these grains during a 10 m.y. interval at 260°C could be *unblocked* by heating to 400°C for 30 minutes in zero magnetic field. Such heating would reset magnetization of these grains to zero.

Now examine points 3 and 4 in Figure 3.21a. These points are on a nomogram connecting τ–T_B conditions for identical grains. (These grains are of course very different from those described by points 1 and 2.)

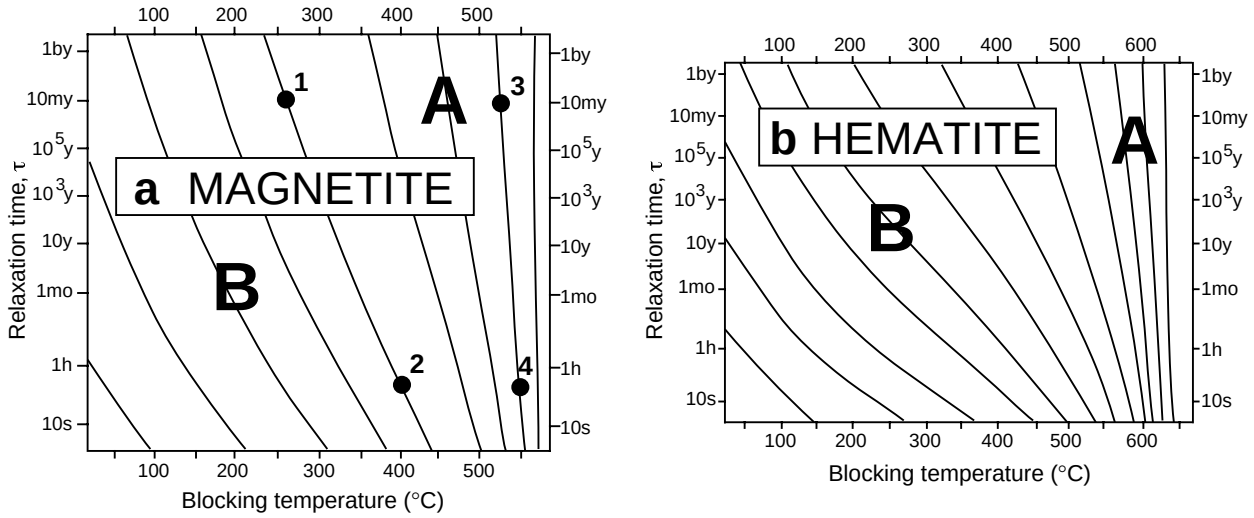

Figure 3.21 Blocking diagrams for (**a**) magnetite and (**b**) hematite. Lines on the diagrams connect combined temperature and relaxation time (τ) conditions that can unblock (reset) the magnetization in a given population of SD grains. See text for explanation. Redrawn from Pullaiah et al. (1975).

Point 3 indicates τ =10 m.y. for T_B = 520°C, whereas point 4 indicates τ = 30 minutes for T_B = 550°C. Thus grains with a 10-m.y. relaxation time at 520°C can be unblocked by heating to only a slightly higher temperature (550°C) for 30 minutes. This is another way of expressing the rapid increase in relaxation time with decreasing temperature for grains with T_B close to the Curie temperature.

The blocking diagrams of Figures 3.21a and 3.21b have been broken into two regions. Grains in the **B** region have blocking temperatures on laboratory time scales (ca. 30 minutes) at temperatures at least 100°C below the Curie temperature. These grains could acquire TVRM at modest temperatures (ca. 300°C) if exposed to those temperatures for geologically reasonable intervals of time (ca. 10 m.y.). Grains in the **B** region are thus unstable carriers of primary components of magnetization and are likely to acquire secondary TVRM or VRM. But grains in the **A** region have laboratory blocking temperatures within 100°C of the Curie temperature. These grains are resistant to resetting of magnetization, except by heating to temperatures approaching the Curie temperature. Grains in the **B** region tend to have blocking temperatures distributed over wide intervals far below the Curie temperature, whereas grains in the **A** region have sharply defined blocking temperatures within 100°C of the Curie temperature. This explains why rocks with T_B dominantly within 100°C of the Curie temperature tend to be stable carriers of primary TRM, whereas rocks with T_B distributed far below the Curie temperature are generally unstable.

Figure 3.21 predicts that primary NRM can survive heating to the greenschist metamorphic range (300°–500°C) but not to the amphibolite range (550°–750°C). Magnetization recorded by magnetite grains with T_B in the **A** region should have magnetization blocked at approximately the same time as radiogenic argon is retained in hornblende (ca. 525°C). However, please be warned that this discussion treats only time-temperature effects. Even low-grade metamorphism is often accompanied by chemical changes that can alter the ferromagnetic minerals, sometimes destroying the primary NRM and/or chemically remagnetizing the rock.

This theory of thermoviscous remanent magnetism also provides a basic theory of thermal demagnetization of secondary NRM. SD grains that have short τ at room temperature also have low T_B while grains with long τ at room temperature have high T_B. Secondary NRM is preferentially carried by the low τ (and low T_B) grains. Thus it is possible to heat a rock to above T_B of grains carrying the secondary NRM but below T_B of grains carrying the primary NRM. This process can be used to erase secondary NRM while leaving the primary NRM essentially unaffected. Procedures for thermal demagnetization will be discussed in detail in Chapter 5.

Caveats and summary

Now for some caveats about why all this theoretical stuff that you've just learned (with some effort but, I hope, little pain) might not, in fact, exactly work. One problem that is often observed is that temperatures required to erase TVRM or VRM components are higher than those predicted by theory. Basic results still apply, but the theory might be optimistic about the predicted ease of removing secondary TVRM. Furthermore, the theory seems to work more dependably for hematite than for magnetite.

Remember that this theory applies to SD grains. A large portion of hematite is SD, while a typical magnetite-bearing rock has a significant portion of its grain-size distribution within the PSD range. It is likely that the presence of PSD grains in magnetite-bearing rocks accounts for some inadequacies of this TVRM theory. Chemical changes in ferromagnetic minerals during metamorphism were also neglected in this TVRM theory. When considering the effects of regional metamorphism or significant burial metamorphism, the strong possibility of chemical change and grain growth must be kept in mind.

Given the distribution of grain sizes and shapes for ferromagnetic grains in rocks, it is expected that some portion of these grains will acquire VRM or TVRM. These components of natural remanent magnetism are generally undesirable secondary components that we seek to destroy during partial demagnetization experiments. We have shown that SD grains with low blocking temperatures are particularly susceptible to acquisition of viscous magnetization. However, it has also been shown that grains with high blocking temperature can retain primary NRM even when other grains in the same rock have acquired VRM. So several components of NRM can reside within different populations of ferromagnetic grains in the same rock. Much paleomagnetic research is concerned with the general problem of deciphering multiple components of magnetization in rocks and uncovering the components of paleomagnetic interest.

ISOTHERMAL REMANENT MAGNETISM (IRM)

Remanent magnetism resulting from short-term exposure to strong magnetizing fields at constant temperature is referred to as *isothermal remanent magnetism* (IRM). In the laboratory, IRM is imparted by exposure (usually at room temperature) to a magnetizing field generated by an electromagnet. IRM is the form of remanence produced in hysteresis experiments and is acquired by ferromagnetic grains with coercive force less than the applied field.

Natural IRM can form as a secondary component of IRM by exposure to transient magnetic fields of lightning strikes. Electrical currents of lightning can exceed 10^4 amperes, and the magnetic field within 1 m of a lightning bolt can be 10^2–10^3 Oe (10–100 mT). It might seem an unlikely circumstance to collect a paleomagnetic sample within 1 m of the location where a lightning bolt has struck. However, a brief examination shows that lightning-induced IRM can be a significant problem, especially in regions of frequent thunderstorm activity.

Worldwide incidence of lightning strikes is a surprising 10^2–10^3 strikes/s. Substantial IRM is acquired within 2 m of a lightning strike, and a reasonable estimate of the time required to erode 2 m from a slope affording a fresh outcrop for paleomagnetic sampling is 10^4 yr. The resulting worldwide average is found to be about 0.1 lightning strike/m^2 over a time interval of 10^4 yr. Considering that lightning storms are concentrated in tropical regions, the probability of lightning strikes having imparted a secondary IRM to outcrops in these regions is substantial. Lightning-prone outcrops on ridges or mesas are likely to have experienced numerous strikes with virtually complete remagnetization. The obvious lesson is to avoid elevated exposures when sampling and to be thorough when examining NRM in the laboratory. Field and laboratory methods are considered in the following chapters.

SUGGESTED READINGS

THERMOREMANENT MAGNETISM:

L. Néel, Some theoretical aspects of rock magnetism, *Adv. Phys.*, v. 4, 191–242, 1955.
***The** classic article on TRM.*

F.D. Stacey, The physical theory of rock magnetism, *Adv. Phys.*, v. 12, 45–133, 1963.
Presents an in-depth investigation of various forms of NRM.

F.D. Stacey and S.K. Banerjee, *The Physical Principles of Rock Magnetism*, Elsevier, Amsterdam, 195 pp, 1974.
Chapters 6 and 7 treat TRM.

DETRITAL REMANENT MAGNETISM:

D.W. Collinson, Depositional remanent magnetization in sediments, *J. Geophys. Res.*, v. 70, 4663–4668, 1965.
Discusses numerous aspects of DRM acquisition.

E. Irving and A. Major, Post-depositional detrital remanent magnetization in a synthetic sediment, *Sedimentology*, v. 3, 135–143, 1964.
A classic PDRM experiment.

F.D. Stacey, On the role of Brownian motion in the control of detrital remanent magnetization of sediments, *Pure Appl. Geophys.*, v. 98, 139–145, 1972.
Treats the Brownian motion model of PDRM.

K.L. Verosub, Depositional and post-depositional processes in the magnetization of sediments, *Rev. Geophys. Space Phys.*, v. 15, 129–143, 1977.
Excellent review article on DRM.

VISCOUS REMANENT MAGNETISM:

D.J. Dunlop, Viscous magnetization of .04–100 μm magnetites, *Geophys. J. R. Astron. Soc.*, v. 74, 667–687, 1983.
A more advanced look at VRM.

G.E. Pullaiah, E. Irving, K.L. Buchan, and D.J. Dunlop, Magnetization changes caused by burial and uplift, *Earth Planet. Sci. Lett.*, v. 28, 133–143, 1975.
Develops the blocking diagram approach to TVRM.

LIGHTNING-INDUCED ISOTHERMAL REMANENT MAGNETISM:

A. Cox, Anomalous remanent magnetization of basalt, *U.S. Geol. Surv. Bull.*, v. 1083–E, 131–160, 1961.
A classic study of effects of lightning on natural remanent magnetism.

PROBLEMS

3.1 Consider a highly elongate rod (needle-shaped grain) of ferromagnetic material.

- **a.** Develop a simple derivation that demonstrates that $N_D \approx 0$ along the long axis of the rod and $N_D \approx 2\pi$ along the diameter of the rod (perpendicular to the long axis).
- **b.** For a needle-shaped grain of titanomagnetite with $j_s = 400$ G, what external magnetic field is required to magnetize the rod to saturation along the diameter (perpendicular to the long axis)?

3.2 A sample is made up of 7% by volume of SD ferromagnetic grains randomly dispersed within a diamagnetic matrix. The coercive force of the ferromagnetic material is dominated by a uniaxial magnetocrystalline anisotropy with anisotropy constant K = 4.5×10^4 erg/cm^3. Saturation magnetization is $j_s = 100$ G.

- **a.** Determine the microscopic coercive force, h_c, of individual SD grains.
- **b.** Consider a hysteresis experiment on this sample. Determine the following hysteresis parameters for the sample: J_s, J_r, H_c.

3.3 Spherical SD grains of hematite (αFe_2O_3) are precipitating from solution at a temperature of 280°K. The microscopic coercive force, $h_c = 10^4$ Oe; the saturation magnetization, $j_s = 2$ G; and the Boltzmann constant, k = 1.38×10^{-16} erg/°K.

- **a.** Use the relaxation time equation (Equation (3.14)) to determine the diameter of spherical hematite grains that have $\tau = 100$ s.

b. Assuming that Equation (3.24) (developed to determine the bias of grain magnetic moments during blocking of TRM) can also be used for CRM formation, what is the bias ($P_+ - P_-$) of grain magnetic moments for a population of spherical hematite grains with the parameters listed above? Assume that CRM is blocked when $\tau = 100$ and that the magnetic field present during precipitation is 1 Oe. Remember that for small x, $\tanh x \approx x$.

3.4 Hydrothermal activity elevates the temperature of a red sandstone to 225°C for a time interval of 1000 yr and results in formation of thermoviscous remanent magnetization (TVRM). If hematite is the exclusive ferromagnetic mineral in this red sandstone, approximately what temperature of thermal demagnetization is required to unblock (remove) this TVRM? The time at maximum temperature during thermal demagnetization is approximately 30 min.